

ELECTRONIC SUPPLEMENTARY INFORMATION

Synthesis, Characterization, and Phosphoesterase Activity of a Series of 4f- and 4d-Sandwich-Type Germanotungstates $[(n\text{-C}_4\text{H}_9)_4\text{N}]_{l/m}\text{H}_2[(\text{M}(\text{H}_2\text{O})_3)(\gamma\text{-GeW}_{10}\text{O}_{35})_2]$ ($\text{M} = \text{Ce}^{\text{III}}, \text{Nd}^{\text{III}}, \text{Gd}^{\text{III}}, \text{Er}^{\text{III}}, l = 7; \text{Zr}^{\text{IV}}, m = 6$)

Elias Tanuhadi[†], Emir Al-Sayed[†], Alexander Roller[‡], Hana Čipčić-Paljetak[⊥], Donatella Verbanac[§] and Annette Rompel^{*, †}

[†] Universität Wien, Fakultät für Chemie, Institut für Biophysikalische Chemie, 1090 Wien, Austria;
www.bpc.univie.ac.at; correspondence to: annette.rompel@univie.ac.at.

[‡] Universität Wien, Fakultät für Chemie, Zentrum für Röntgenstrukturanalyse, 1090 Wien, Austria.

[⊥] Center for Translational and Clinical Research, Croatian Center of Excellence for Reproductive and Regenerative Medicine, School of Medicine, University of Zagreb, 10000 Zagreb, Croatia.

[§] Faculty of Pharmacy and Biochemistry, University of Zagreb, 10000 Zagreb, Croatia.

Content

1. General Information	3
2. Experimental Procedure	4
2.1. Preparation of $(C_{16}H_{36}N)_7H_2[Ce(H_2O)_3(GeW_{10}O_{35})_2] \cdot 3(CH_3)_2CO$ $[Ce(H_2O)_3(GeW_{10})_2]^{9-}$	4
2.2. Preparation of $(C_{16}H_{36}N)_7H_2[Nd(H_2O)_3(GeW_{10}O_{35})_2] \cdot 3(CH_3)_2CO$ $[Nd(H_2O)_3(GeW_{10})_2]^{9-}$	4
2.3. Preparation of $(C_{16}H_{36}N)_7H_2[Gd(H_2O)_3(GeW_{10}O_{35})_2] \cdot 3(CH_3)_2CO$ $[Gd(H_2O)_3(GeW_{10})_2]^{9-}$	4
2.4. Preparation of $(C_{16}H_{36}N)_7H_2[Er(H_2O)_3(GeW_{10}O_{35})_2] \cdot 3(CH_3)_2CO$ $[Er(H_2O)_3(GeW_{10})_2]^{9-}$	4
2.5. Preparation of $(C_{16}H_{36}N)_6H_2[Zr(H_2O)_3(GeW_{10}O_{35})_2] \cdot 3(CH_3)_2CO$ $[Zr(H_2O)_3(GeW_{10})_2]^{8-}$	4
2.6. Ion exchange procedure for $[Ce(H_2O)_3(GeW_{10})_2]^{9-}$	5
2.7. Ion exchange procedure for $[Zr(H_2O)_3(GeW_{10})_2]^{8-}$	5
3. IR-spectra	10
4. Thermogravimetric Analysis	14
5. Single-Crystal X-ray Diffraction	18
6. Powder X-ray Diffraction (PXRD).....	23
7. UV-Vis Spectroscopy.....	24
8. Hydrolysis Studies	26
8.1. Hydrolysis experiments on 4-nitrophenylphosphate (NPP):	26
8.2. Hydrolysis experiments on O,O-dimethyl O-(4-nitrophenyl) phosphate (DMNP):	26
8.3. Recyclability experiment on $[Zr(H_2O)_3(GeW_{10}O_{35})_2]^{8-}$	26
9. Antibacterial Activity	37
10. References	39

1. General Information

All reagents and chemicals were of high-purity grade and were used as purchased without further purification. $[(n\text{-C}_4\text{H}_9)_4\text{N}]_4[\gamma\text{-GeW}_{10}\text{O}_{34}(\text{H}_2\text{O})_2]$ was prepared according to the literature procedure reported by Sugahara *et al.*¹

Elemental analysis: Elemental analysis of Ce, Nd, Gd, Er, Zr and W contents was performed with an iCAP 6500 series inductively coupled plasma-optical emission spectrometry (ICP-OES) spectrometer (Thermo Scientific, USA). The ICP-OES was equipped with a standard sample introduction system consisting of a concentric nebulizer and a cyclonic spray chamber. Transportation of sample solutions was performed by the peristaltic pump of the iCAP 6500 coupled to an ASX-520 auto sampler (Cetac, USA). Per element two sensitive and non-interfered emission lines were used, the first line for measurement and the second line for quality control. Elemental microanalysis of C/H/N/O contents was performed by Mikroanalytisches Laboratorium (University Vienna, Faculty of Chemistry). An EA 3000 (Eurovector) was used for C/H/N/S-analysis. O-determination was performed by high temperature digestion using the HT 1500 (Hekatech, Germany) pyrolysis system in combination with the EA 3000 system.

Attenuated total reflection Fourier-transform Infrared Spectroscopy: All spectra were recorded on a Bruker Tensor 27 IR Spectrometer equipped with a single-reflection diamond-ATR unit. Frequencies are given in cm^{-1} , intensities denoted as w = weak, m = medium, s = strong.

Thermogravimetric analysis (TGA): was performed on a Mettler SDTA851e Thermogravimetric Analyzer under N_2 flow with a heating rate of 5 K min⁻¹ in the region 298–1023 K.

Single crystal X-ray diffraction (SXRD): The X-ray data were measured on a Bruker D8 VENTURE equipped with a multilayer monochromator, Mo K α Incoatec Microfocus sealed tube, and Kryoflex cooling device equipped with multilayer monochromators, Mo K α ($\lambda=0.71073\text{\AA}$) INCOATEC micro focus sealed tubes. The structures were solved by direct methods and refined by full-matrix least-squares. Non hydrogen atoms were refined with anisotropic displacement parameters. The following software was used for the structure-solving procedure: frame integration, Bruker SAINT software package using a narrow-frame algorithm (absorption correction)², SADABS³, SHELXS-2013⁴ (structure solution), SHELXL-2013⁵ (refinement), OLEX2⁶ (structure solution, refinement, molecular diagrams and graphical user-interface), and SHELXLE⁷ (molecular diagrams and graphical user interface). Experimental data and CCDC-codes are provided in **Tables S7-S17**.

Powder X-ray diffraction was performed on an EMPYREAN diffractometer system using Cu K α radiation ($\lambda = 1.540598$), a PIXcel3D-Medipix3 1 × 1 detector (used as a scanning line detector) and a divergence slit fixed at 0.1 mm. The scan range was from 5° to 50° (2 θ).

Solubility: The solubility of the anions was determined by weighing a defined amount of sample (10 mg) into an Eppendorf tube and addition of the corresponding solvent in 50 μL steps. Once the compound was completely dissolved the sample was centrifuged at 10000 rpm for 60 seconds and further checked for undissolved solids under the microscope.

UV-Vis spectroscopy: UV-Vis spectra were collected on a Shimadzu UV 1800 spectrophotometer.

Minimum inhibitory concentrations (MICs) were determined by the broth microdilution method according to guidelines of the Clinical Laboratory Standards Institute.⁸ Double dilutions of tested compounds in 96-well microtiter plates were prepared in 256-0.5 mg/mL concentration range. *M. catarrhalis* was grown on Columbia agar with 5% sheep blood. Inocula were prepared by direct colony suspension method and plates inoculated with 5×10^4 CFU/well. Results were determined by visual inspection after 20-22 h incubation at 37°C in ambient air. Testing was performed by the standard broth microdilution method with azithromycin and ciprofloxacin as the reference antibiotics to assess test validity.

2. Experimental Procedure

2.1. Preparation of $(C_{16}H_{36}N)_7H_2[Ce(H_2O)_3(GeW_{10}O_{35})_2] \cdot 3(CH_3)_2CO$ [$Ce(H_2O)_3(GeW_{10})_2]^{9-}$

To a stirred solution of $[(n-C_4H_9)_4N]_4[\gamma-GeW_{10}O_{34}(H_2O)_2]$ (250 mg, 0.072 mmol) in acetone/water (5 mL/80 μ L) was added $[Ce(acac)_3]$ (15.75 mg, 0.036 mmol, 0.5 equiv. with respect to $(TBA)[GeW_{10}]$) and the resulting solution was stirred for 90 min at RT (about 20°C). Orange block shaped crystals of $[Ce(H_2O)_3(GeW_{10})_2]^{9-}$ were obtained after approximately one week from a mixture of acetone and diethyl ether (~1.25 mL). Yield: 199 mg, 79 % based on Ce. Elemental analysis calcd. (found) for $C_{121}H_{278}N_7O_{74}CeGe_2W_{20}$ ($(TBA)_7H_2[Ce(H_2O)_3(GeW_{10}O_{35})_2] \cdot 3(CH_3)_2CO$): C 20.83 (19.07), H 4.02 (3.75), N 1.41 (1.48), O 16.97 (16.78), Ge 2.08 (2.14), W 52.69 (51.6), Ce 2.01 (2.07).

2.2. Preparation of $(C_{16}H_{36}N)_7H_2[Nd(H_2O)_3(GeW_{10}O_{35})_2] \cdot 3(CH_3)_2CO$ [$Nd(H_2O)_3(GeW_{10})_2]^{9-}$

The synthetic procedure for $[Nd(H_2O)_3(GeW_{10})_2]^{9-}$ is similar to that of $[Ce(H_2O)_3(GeW_{10})_2]^{9-}$ except that $[Ce(acac)_3]$ was replaced by $[Nd(acac)_3]$ (15.89 mg, 0.036 mmol). Blue block shaped crystals of $[Nd(H_2O)_3(GeW_{10})_2]^{9-}$ were obtained after approximately one week from a mixture of acetone and diethyl ether (~1.3 mL). Yield: 190 mg, 76 % based on Nd. Elemental analysis calcd. (found) for $C_{121}H_{278}N_7O_{74}NdGe_2W_{20}$ ($(TBA)_7H_2[Nd(H_2O)_3(GeW_{10}O_{35})_2] \cdot 3(CH_3)_2CO$): C 20.82 (18.99), H 4.01 (3.67), N 1.40 (1.46), O 16.96 (16.25), Ge 2.08 (2.11), W 52.66 (50.90), Nd 2.07 (2.09).

2.3. Preparation of $(C_{16}H_{36}N)_7H_2[Gd(H_2O)_3(GeW_{10}O_{35})_2] \cdot 3(CH_3)_2CO$ [$Gd(H_2O)_3(GeW_{10})_2]^{9-}$

The synthetic procedure for $[Gd(H_2O)_3(GeW_{10})_2]^{9-}$ is similar to that of $[Ce(H_2O)_3(GeW_{10})_2]^{9-}$ except that $[Ce(acac)_3]$ was replaced by $[Gd(acac)_3]$ (16.4 mg, 0.036 mmol). Colorless block shaped crystals of $[Gd(H_2O)_3(GeW_{10})_2]^{9-}$ were obtained after approximately one week from a mixture of acetone and diethyl ether (~1.5 mL). Yield: 135 mg, 54 % based on Gd. Elemental analysis calcd. (found) for $C_{121}H_{278}N_7O_{74}GdGe_2W_{20}$ ($(TBA)_7H_2[Gd(H_2O)_3(GeW_{10}O_{35})_2] \cdot 3(CH_3)_2CO$): C 20.78 (18.91), H 4.01 (3.70), N 1.40 (1.44), O 16.93 (17.35), Ge 2.08 (2.11), W 52.56 (50.80), Gd 2.25 (2.00).

2.4. Preparation of $(C_{16}H_{36}N)_7H_2[Er(H_2O)_3(GeW_{10}O_{35})_2] \cdot 3(CH_3)_2CO$ [$Er(H_2O)_3(GeW_{10})_2]^{9-}$

The synthetic procedure for $[Er(H_2O)_3(GeW_{10})_2]^{9-}$ is similar to that of $[Ce(H_2O)_3(GeW_{10})_2]^{9-}$ except that $[Ce(acac)_3]$ was replaced by $[Er(acac)_3]$ (16.4 mg, 0.036 mmol). Light pink block shaped crystals of $[Er(H_2O)_3(GeW_{10})_2]^{9-}$ were obtained after approximately one week from a mixture of acetone and diethyl ether (~1.3 mL). Yield: 101 mg, 40 % based on Er. Elemental analysis calcd. (found) for $C_{121}H_{278}N_7O_{74}ErGe_2W_{20}$ ($(TBA)_7H_2[Er(H_2O)_3(GeW_{10}O_{35})_2] \cdot 3(CH_3)_2CO$): C 20.76 (17.89), H 4.00 (3.53), N 1.40 (1.36), O 16.90 (16.88), Ge 2.07 (2.18), W 52.49 (52.10), Er 2.39 (2.34).

2.5. Preparation of $(C_{16}H_{36}N)_6H_2[Zr(H_2O)_3(GeW_{10}O_{35})_2] \cdot 3(CH_3)_2CO$ [$Zr(H_2O)_3(GeW_{10})_2]^{8-}$

To a stirred solution of $[\text{Zr}(\text{acac})_4]$ (72 mg, 0.14 mmol, 2.0 equiv. with respect to $(\text{TBA})[\text{GeW}_{10}]$) in 5 mL acetone H_2O_2 (80 μL , 30 %) was added. After stirring the yellow reaction mixture for 5 min, $[(n\text{-C}_4\text{H}_9)_4\text{N}]_4[\gamma\text{-GeW}_{10}\text{O}_{34}(\text{H}_2\text{O})_2]$ (250 mg, 0.072 mmol) was added. The resulting solution was stirred for 90 min at RT (about 20°C). Colorless block shaped crystals of $[\text{Zr}(\text{H}_2\text{O})_3(\text{GeW}_{10})_2]^{8-}$ were obtained after approximately one week from a mixture of acetone and diethyl ether (~1.25 mL). Yield: 310 mg, 65 % based on W. Elemental analysis calcd. (found) for $\text{C}_{105}\text{H}_{236}\text{N}_6\text{O}_{73}\text{ZrGe}_2\text{W}_{20}$ $((\text{TBA})_6\text{H}_2[\text{Zr}(\text{H}_2\text{O})_3(\text{GeW}_{10}\text{O}_{35})_2] \cdot 3(\text{CH}_3)_2\text{CO})$: C 18.92 (18.99), H 3.57 (3.71), N 1.26 (1.39), O 17.53 (17.56), Ge 2.18 (1.36), W 55.17 (51.6), Zr 1.37 (1.38).

2.6. Ion exchange procedure for $[\text{Ce}(\text{H}_2\text{O})_3(\text{GeW}_{10})_2]^{9-}$

$[\text{Ce}(\text{H}_2\text{O})_3(\text{GeW}_{10})_2]^{9-}$ (346 mg, 0.0522 mmol) was dissolved in acetonitrile (2.5 mL) and the resulting solution was added dropwise to a stirred acetonitrile (2.5 mL) solution of NaClO_4 (586 mg, 0.4688 mmol). The resulting reaction mixture was stirred at room temperature for 90 min giving a yellow precipitate which was washed with generous amounts of cold acetonitrile (~10 mL) and air dried. Yield: 80 mg, 29 % based on tungsten.

2.7. Ion exchange procedure for $[\text{Zr}(\text{H}_2\text{O})_3(\text{GeW}_{10})_2]^{8-}$

The procedure for $[\text{Zr}(\text{H}_2\text{O})_3(\text{GeW}_{10})_2]^{8-}$ is similar to that of $[\text{Ce}(\text{H}_2\text{O})_3(\text{GeW}_{10})_2]^{9-}$ except that $[\text{Ce}(\text{H}_2\text{O})_3(\text{GeW}_{10})_2]^{9-}$ was replaced by $[\text{Zr}(\text{H}_2\text{O})_3(\text{GeW}_{10})_2]^{8-}$ (347 mg, 0.0522 mmol). Yield: 160 mg, 60 % based on tungsten.

Table S1. Survey of existing reaction systems using lacunary POM precursors in organic media. DMF = N, N – dimethyl formamide, DMSO = dimethylsulfoxide, OAc = acetate, TBA = tetrabutyl ammonium $[(n\text{-C}_4\text{H}_9)_4\text{N}]^+$.

Building block	Heteroatom	Solvent	Sum formula	Ref.
$\text{TBA}_4\text{H}_4[\gamma\text{-SiW}_{10}\text{O}_{36}]\cdot 2\text{H}_2\text{O}$	Zn ²⁺	acetone/H ₂ O	TBA ₈ [{Zn ₂ W(O)O ₃) ₂ H ₄ {α-SiW ₉ O ₃₃ } ₂]•5H ₂ O	9
			TBA ₈ [{Zn ₂ W(O)O ₃) ₂ H ₄ {β-SiW ₉ O ₃₃ } ₂]•7H ₂ O	
			TBA ₈ [{Zn(OH ₂)(μ ₃ -OH)} ₂ {Zn(OH ₂) ₂ }•γ-HSiW ₁₀ O ₃₆ } ₂]•9H ₂ O	
	Co ²⁺ , Zn ²⁺	acetone/H ₂ O/EtOAc	TBA ₈ [{Co(OH ₂)(μ ₃ -OH)} ₂ {Zn(OH ₂) ₂ }•HSiW ₁₀ O ₃₆ } ₂]•2.5EtOAc•12H ₂ O	10
	Ni ²⁺ , Zn ²⁺		TBA ₈ [{Ni(OH ₂)(μ ₃ -OH)} ₂ {Zn-(OH ₂) ₂ }•HSiW ₁₀ O ₃₆ } ₂]•5EtOAc•12H ₂ O	
	Zn ²⁺		TBA ₈ [{Zn(OH ₂)(μ ₃ -OH)} ₂ {Zn(OH ₂) ₂ }•HSiW ₁₀ O ₃₆ } ₂]•5 EtOAc•12H ₂ O	
	Cu ²⁺	acetone /acetamide	TBA ₈ [Cu(γ-SiW ₁₀ O ₃₄) ₂ (CH ₃ CONH) ₂]•4H ₂ O	11
		acetone	TBA ₈ H ₄ [Cu ₂ (γ-SiW ₁₀ O ₃₆) ₂ H ₂ O]•11H ₂ O•CH ₃ COCH ₃	
		ACN	TBA ₈ H ₂ [Cu ₄ (γ-SiW ₁₀ O ₃₆) ₂ (CH ₃ COO) ₂]•5H ₂ O	
	Ln = Y ³⁺ , Nd ³⁺ , Eu ³⁺ , Gd ³⁺ , Tb ³⁺ , Dy ³⁺	acetone/HNO ₃	TBA ₆ H ₄ [{Ln(H ₂ O) ₂ (acetone)} ₂ {γ-SiW ₁₀ O ₃₆ } ₂]•n(acetone)•2H ₂ O	12
	Pd ²⁺	acetone/H ₂ O	TBA ₄ [γ-H ₂ SiW ₁₀ O ₃₆ Pd ₂ (OAc) ₂]	13
			[{(n-C ₅ H ₁₁) ₄ N}] ₄ [γ-H ₂ SiW ₁₀ O ₃₆ Pd ₂ (OAc) ₂]	
	Ag ⁺	acetone/DMSO	TBA ₈ [Ag ₄ (DMSO) ₂ (γ-HSiW ₁₀ O ₃₆) ₂]•2DMSO•2H ₂ O	14
	Y ³⁺	acetone	TBA ₈ H ₂ [{γ-SiYW ₁₀ O ₃₆ } ₂]•7H ₂ O	15
	Co ²⁺	DMF/acetone	{Co(DMF) ₂ (H ₂ O) ₃ }•{Co(DMF) ₄ (H ₂ O)}[γ-SiW ₁₀ O ₃₄ (DMF) ₂]•2DMF•11H ₂ O	16
		DMF	TBA ₆ [Co ₂ (γ-H ₃ SiW ₁₀ O ₃₆) ₂]•3H ₂ O	
		acetone	TBA ₆ [{Co(H ₂ O) ₂ (μ ₃ -OH) ₂₂ O) ₂ }•γ-H ₂ SiW ₁₀ O ₃₆ } ₂]•5H ₂ O	
	Ag ⁺		TBA ₈ [Ag ₆ (γ-H ₂ SiW ₁₀ O ₃₆) ₂]•5H ₂ O	17
	Co ²⁺	acetone/H ₂ O	TBA ₈ H ₂ [{Co(H ₂ O) ₂ (μ ₃ -OH) ₂₂ O) ₂ }•γ-SiW ₁₀ O ₃₆ } ₂]•13H ₂ O	18
		acetone	TBA ₈ H ₄ [{Co ₄ (μ ₃ -OH) ₄ }•γ-SiW ₁₀ O ₃₆ } ₂]•5H ₂ O	
	Ce ³⁺		TBA ₆ [{Ce(H ₂ O) ₂ }•{Ce(CH ₃ CN) ₂ }•{μ ₄ -O}(γ-SiW ₁₀ O ₃₆) ₂]•4H ₂ O	19
$\text{TBA}_4\text{H}_6[\text{A-}\alpha\text{-SiW}_9\text{O}_{34}]\cdot 2\text{H}_2\text{O}$	Fe ³⁺	acetone/H ₂ O	TBA ₇ H ₁₀ [Fe(SiW ₉ O ₃₄) ₂]•2H ₂ O•C ₂ H ₄ Cl ₂	20
	Co ²⁺		TBA ₇ H ₁₁ [Co(SiW ₉ O ₃₄) ₂]•2H ₂ O•C ₂ H ₄ Cl ₂	
	Mn ³⁺		TBA ₇ H ₁₀ [Mn(SiW ₉ O ₃₄) ₂]•3H ₂ O	
	Sn ²⁺	1,2-dichloroethane	TBA ₇ H[Sn ₆ (A-α-SiW ₉ O ₃₄) ₂]•2H ₂ O	21
	Sn ²⁺ /Sn ⁴⁺	nitromethane/1,2-dichloroethane	TBA ₇ H[Sn ₃ Sn ₃ (μ ₃ -O) ₃ (A-α-SiW ₉ O ₃₄) ₂]•3H ₂ O	
	Bi ³⁺	1,2-dichloroethane	TBA ₇ [Bi ₂ (A-α-SiW ₉ O ₃₂) ₂ (OAc)(H ₂ O) ₂]•3C ₂ H ₄ Cl ₂ •2H ₂ O	22

		acetone	TBA ₈ H ₂ [Bi ₂ (γ-SiW ₁₀ O ₃₆) ₂]•4H ₂ O TBA ₇ [Bi ₄ O(γ-SiW ₁₀ O ₃₆) ₂ (OAc)]•2CH ₃ COCH ₃ •H ₂ O	
	M = Fe ³⁺ , Co ²⁺ , Ni ²⁺ , Cu ²⁺ , Ga ³⁺	acetone/H ₂ O	TBA ₇ H _n [MMn ₄ (OH) ₂ (A-α-SiW ₉ O ₃₄) ₂]•2H ₂ O•C ₂ H ₄ Cl ₂	23
	M = Mn ³⁺ , Cu ²⁺ ; Ln = Gd ³⁺ , Dy ³⁺ , Lu ³⁺ ; L = acac (acetylacetone)	1,2-dichloroethane	TBA _n H _m [FeM ₄ {Ln(L) ₂ } ₂ O ₂ (A-α-SiW ₉ O ₃₄) ₂]	24
	Ag ⁺	acetone/H ₂ O/DMF	TBA ₁₆ (Me ₂ NH) ₈ H ₅ Ag ₂ [Ag ₂₇ (Si ₂ W ₁₈ O ₆₆) ₃]•12C ₃ H ₄ O ₃ •34H ₂ O	25
TBA ₄ [A-α-GeW ₉ O ₂₈ (OCH ₃) ₆]	Fe ³⁺	acetone/H ₂ O	TBA ₇ H ₁₀ [(A-α-GeW ₉ O ₃₄) ₂ Fe]	26
TBA ₄ N] ₄ [γ-GeW ₁₀ O ₃₄ (H ₂ O) ₂]	M = Ce ³⁺ , Nd ³⁺ , Gd ³⁺ , Er ³⁺ , Zr ⁴⁺ ; n = 6, 7	acetone/H ₂ O//acetone/H ₂ O ₂	(TBA) _n H ₂ [(M(H ₂ O) ₃)(γ-GeW ₁₀ O ₃₅) ₂]	this work

Table S2. Survey of existing crystal structures of 4f- and Zr⁴⁺-doped germanotungstates. GeW₁₁ = K₈[β₂-GeW₁₁O₃₉] • 14H₂O, GeW₁₀ = K₈[γ-GeW₁₀O₃₆] • 6H₂O. enMe = 1,2-diaminopropane, en = ethylenediamine, D-tartH₄ = D-tartaric acid, glyH₂ = glycolic acid, OAc = acetate, tris = tris(hydroxymethyl)aminomethane.

Formula	Germanotungstate building block present in structure	Number & types of M centres	Ref.
[Eu ₄ (H ₂ O) ₁₈ Ge ₂ W ₂₂ O ₇₈] ⁴⁻ •16.5H ₂ O	β ₂ - GeW ₁₁	4 Ln ³⁺ (Ln = Eu)	27
[Eu(H ₂ O) ₂ GeW ₁₁ O ₃₉] ⁵⁻ •10H ₂ O	β ₂ - GeW ₁₁	1 Ln ³⁺ (Ln = Eu)	27
[Ln(α-GeW ₁₁ O ₃₉) ₂] ¹³⁻	α - GeW ₁₁	1 Ln ³⁺ (Ln = La, Ce)	28
[{Ln(μ-CH ₃ COO)GeW ₁₁ O ₃₉ (H ₂ O)} ₂] ¹²⁻	α - GeW ₁₁	1 Ln ³⁺ (Ln = Pr, Nd, Sm, Eu, Gd, Tb, Dy, Ho, Er, Tm, Yb)	28
[{Ln(CH ₃ COO)GeW ₁₁ O ₃₉ (H ₂ O)} ₂] ¹²⁻	α - GeW ₁₁	1 Ln ³⁺ (Ln = Eu, Gd, Tb, Dy, Ho, Er, Tm, Yb)	29
[Ln(GeW ₁₁ O ₃₉)(H ₂ O) ₂] ¹⁰⁻ •nH ₂ O	α - GeW ₁₁	1 Ln ³⁺ (Ln = Nd, Tb, Eu)	30

$[\text{Pr}_{1.5}(\text{GeW}_{11}\text{O}_{39})(\text{H}_2\text{O})_{5.75}]^{3.5} \bullet n\text{H}_2\text{O}$	$\alpha - \text{GeW}_{11}$	$1 \text{ Ln}^{3+} (\text{Ln} = \text{Pr})$	31
$[\text{La}(\text{H}_2\text{O})_2(\text{GeW}_{11}\text{O}_{39})]_2^{10-} \bullet 7\text{H}_2\text{O}$	$\alpha - \text{GeW}_{11}$	$1 \text{ Ln}^{3+} (\text{Ln} = \text{La})$	32
$[\text{La}(\text{H}_2\text{O})_3(\text{GeW}_{11}\text{O}_{39})]_2^{26-} \bullet 38\text{H}_2\text{O}$	$\alpha - \text{GeW}_{11}$	$1 \text{ Ln}^{3+} (\text{Ln} = \text{La})$	32
$\text{Ln}/[\alpha\text{-GeW}_{11}\text{O}_{39}]^{3-}$	$\alpha - \text{GeW}_{11}$	$1 \text{ Ln}^{3+} (\text{Ln} = \text{Nd, Sm, Y, Yb})$	33
$[\text{Ln}_4(\alpha(1,4)\text{GeW}_{10}\text{O}_{38})_2(\text{H}_2\text{O})_6]^{12-} \bullet n\text{H}_2\text{O}$	$\alpha - \text{GeW}_{11}$	$1 \text{ Ln}^{3+} (\text{Ln} = \text{Dy, Er})$	34
$[\text{Ln}(\text{GeW}_{11}\text{O}_{39})_2]^{13-}$	$\alpha/\beta_2 - \text{GeW}_{11}$	$1 \text{ Ln}^{3+} (\text{Ln} = \text{La, Ce, Pr, Nd, Sm, Gd, Dy; Ho, Er, Tm})$	35
$[\text{Ln}_{12}(\text{OH})_{12}(\text{H}_2\text{O})_{18}\text{Ge}_n(\text{GeW}_{10}\text{O}_{38})_6]^{n-}$	$\beta - (4, 11)\text{-GeW}_{10}$	$12 \text{ Ln}^{3+} (\text{Ln} = \text{Eu, Gd, Dy})$	36
$[\text{Ln}_4(\text{H}_2\text{O})_6(\beta\text{-GeW}_{10}\text{O}_{38})_2]^{12-}$	$\alpha/\beta - (1, 5)\text{-GeW}_{10}$ $\alpha/\beta - (1, 8)\text{-GeW}_{10}$	$4 \text{ Ln}^{3+} (\text{Ln} = \text{Gd, Tb, Dy, Ho, Er, Tm, Yb, Lu})$	37
$[(\text{Ln}_{12}\text{Ge}_6\text{W}_{60}\text{O}_{228}(\text{H}_2\text{O})_{24})_n] \bullet n\text{H}_2\text{O}$	$\alpha/\beta - (1, 5)\text{-GeW}_{10}$ $\alpha/\beta - (1, 8)\text{-GeW}_{10}$	$12 \text{ Ln}^{3+} (\text{Ln} = \text{Pr, Nd, Sm})$	38
$[(\text{Ln}_{12}\text{Ge}_6\text{W}_{60}\text{O}_{228}(\text{H}_2\text{O})_{24})_2] \bullet n\text{H}_2\text{O}$	$\alpha/\beta - (1, 5)\text{-GeW}_{10}$ $\alpha/\beta - (1, 8)\text{-GeW}_{10}$	$24 \text{ Ln}^{3+} (\text{Ln} = \text{Nd, Pr})$	38
$[\text{K}_8\text{Ce}_{24}\text{Ge}_{12}\text{W}_{120}\text{O}_{456}(\text{OH})_{12}(\text{H}_2\text{O})_{64}]^{52-}$	$\alpha/\beta - (1, 5)\text{-GeW}_{10}$ $\alpha/\beta - (1, 8)\text{-GeW}_{10}$	$24 \text{ Ln}^{3+} (\text{Ln} = \text{Ce})$	39
$[\text{Ln}_4(\text{H}_2\text{O})_6(\beta\text{-GeW}_{10}\text{O}_{38})_2]^{12-}$	$\alpha/\beta - (1, 5)\text{-GeW}_{10}$ $\alpha/\beta - (1, 8)\text{-GeW}_{10}$	$4 \text{ Ln}^{3+} (\text{Ln} = \text{Dy, Ho, Er, Tm})$	37
$[\text{Ce}_{20}\text{Ge}_{10}\text{W}_{100}\text{O}_{376}(\text{OH})_4(\text{H}_2\text{O})_{30}]^{56-} \bullet 180\text{H}_2\text{O}$	$\alpha/\beta - (1, 5)\text{-GeW}_{10}$ $\alpha/\beta - (1, 8)\text{-GeW}_{10}$	$20 \text{ Ln}^{3+} (\text{Ln} = \text{Ce})$	40
$[(A\text{-}\alpha\text{-GeW}_9\text{O}_{34})_2(\text{LnOH}_2)_3\text{CO}_3]^{13-}$	$A\text{-}\beta\text{-GeW}_9\text{O}_{34}$	$3 \text{ Ln}^{3+} (\text{Ln} = \text{Y, Sm, Yb})$	41
$[\text{Zr}_2(\text{O}_2)_2(\text{GeW}_{11}\text{O}_{39})_2]^{12-}$	$\alpha - \text{GeW}_{11}$	1 Zr^{4+}	42
$[\text{Zr}_3\text{O}(\text{OH})_2(\alpha\text{-GeW}_9\text{O}_{34})(\beta\text{-GeW}_9\text{O}_{34})]^{12-}$	$A\text{-}\beta\text{-GeW}_9\text{O}_{34}$	3 Zr^{4+}	43
$[\text{Zr}_{24}\text{O}_{22}(\text{OH})_{10}(\text{H}_2\text{O})_2(\text{W}_2\text{O}_{10}\text{H})_2(\text{GeW}_9\text{O}_{34})_4(\text{GeW}_8\text{O}_{31})_2]^{32-}$	$B\text{-}\alpha\text{-GeW}_9\text{O}_{34}, B\text{-}\alpha\text{-GeW}_8\text{O}_{31}$	24 Zr^{4+}	44
$[\text{Zr}_4(\mu_3\text{-O})_2(\mu\text{-OH})_2(\text{enMe})_2(\text{B}\text{-}\alpha\text{-GeW}_{10}\text{O}_{37})_2]^{14-} / [\text{Zr}_4(\mu_3\text{-O})_2(\mu\text{-OH})_2(\text{en})_2(\text{B}\text{-}\alpha\text{-GeW}_{10}\text{O}_{37})_2]^{14-}$	$B\text{-}\alpha\text{-GeW}_{10}$	4 Zr^{4+}	45

$[\text{Zr}_4(\text{H}_2\text{O})_2(\mu\text{-OH})(\mu_3\text{-O})_2(\text{D-tartH})(\text{GeW}_{10}\text{O}_{37})_2]^{12-} / [\text{Zr}_4(\text{H}_2\text{O})_2(\mu_3\text{-O})_2(\text{gly})_2(\text{GeW}_{10}\text{O}_{37})_2]^{12-}$	$\beta\text{-GeW}_{10}$	4 Zr^{4+}	46
$[\text{Zr}_4(\mu_3\text{-O})_2(\text{OH})_2(\text{OAc})_2(\alpha\text{-GeW}_{10}\text{O}_{37})_2]^{12-} / [\text{Zr}_6(\mu_3\text{-O})_3(\text{OH})_3(\text{OAc})(\text{H}_2\text{O})(\beta\text{-GeW}_{10}\text{O}_{37})_3]^{16-} / [\{\text{Zr}_5(\mu_3\text{-OH})_4(\text{OH})_2\}@\{\text{Zr}_2(\text{OAc})_2(\alpha\text{-GeW}_{10}\text{O}_{38})_2\}_2]^{22-}$	$\alpha/\beta\text{-GeW}_{10}$	$4 \text{ Zr}^{4+}/6 \text{ Zr}^{4+}/9 \text{ Zr}^{4+}$	47
$[\text{Zr}_4(\mu_3\text{-O})_2(\text{tris})_2(\alpha\text{-GeW}_{10}\text{O}_{37})_2]^{12-}$	$\alpha\text{-GeW}_{10}$	4 Zr^{4+}	48
$(\text{TBA})_n\text{H}_2[(\text{M}(\text{H}_2\text{O})_3)(\gamma\text{-GeW}_{10}\text{O}_{35})_2]$	$[(n\text{-C}_4\text{H}_9)_4\text{N}]_4[\gamma\text{-Ge}^{\text{IV}}\text{W}_{10}\text{O}_{34}(\text{H}_2\text{O})_2]$	$1 \text{ M}^{n+} (\text{M} = \text{Ce}^{3+}, \text{Nd}^{3+}, \text{Gd}^{3+}, \text{Er}^{3+}, \text{Zr}^{4+})$	this work

3. IR-spectra

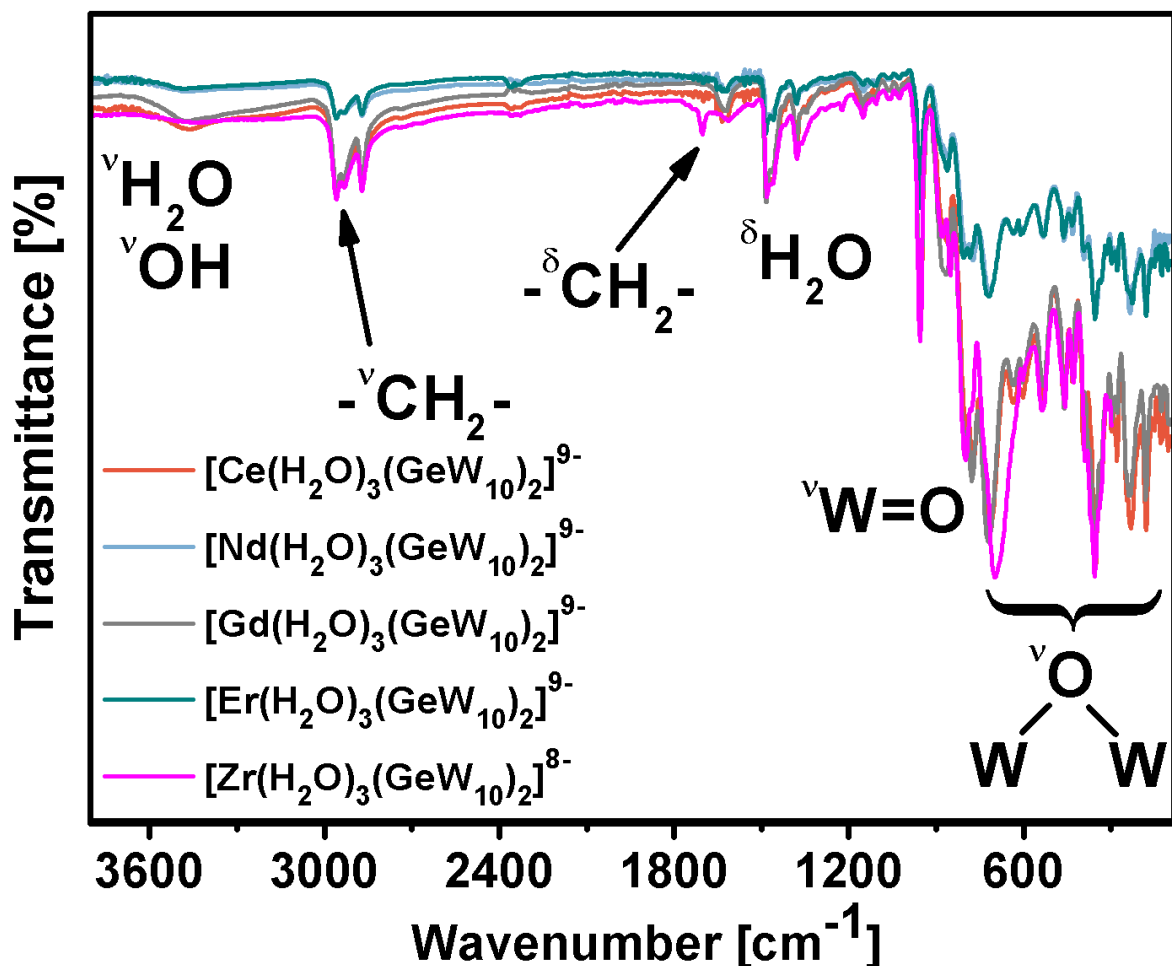


Figure S1. IR-spectra of $(C_{16}H_{36}N)_7H_2[M(GeW_{10}O_{35})_2]$ ($M = Ce^{III}, Nd^{III}, Gd^{III}, Er^{III}, Zr^{IV}$). $[Ce^{III}(H_2O)_3(GeW_{10})_2]^{9-}$ (ATR-IR, cm^{-1}): 3364.2 (s), 3206.7 (s), 1634.9 (m), 1530.3 (m), 1394.5 (m), 1326.9 (w), 1243.9 (w), 1153.9 (w), 1019.0 (w), 935.9 (w), 748.3 (w), 628.0 (w), 507.8 (w).

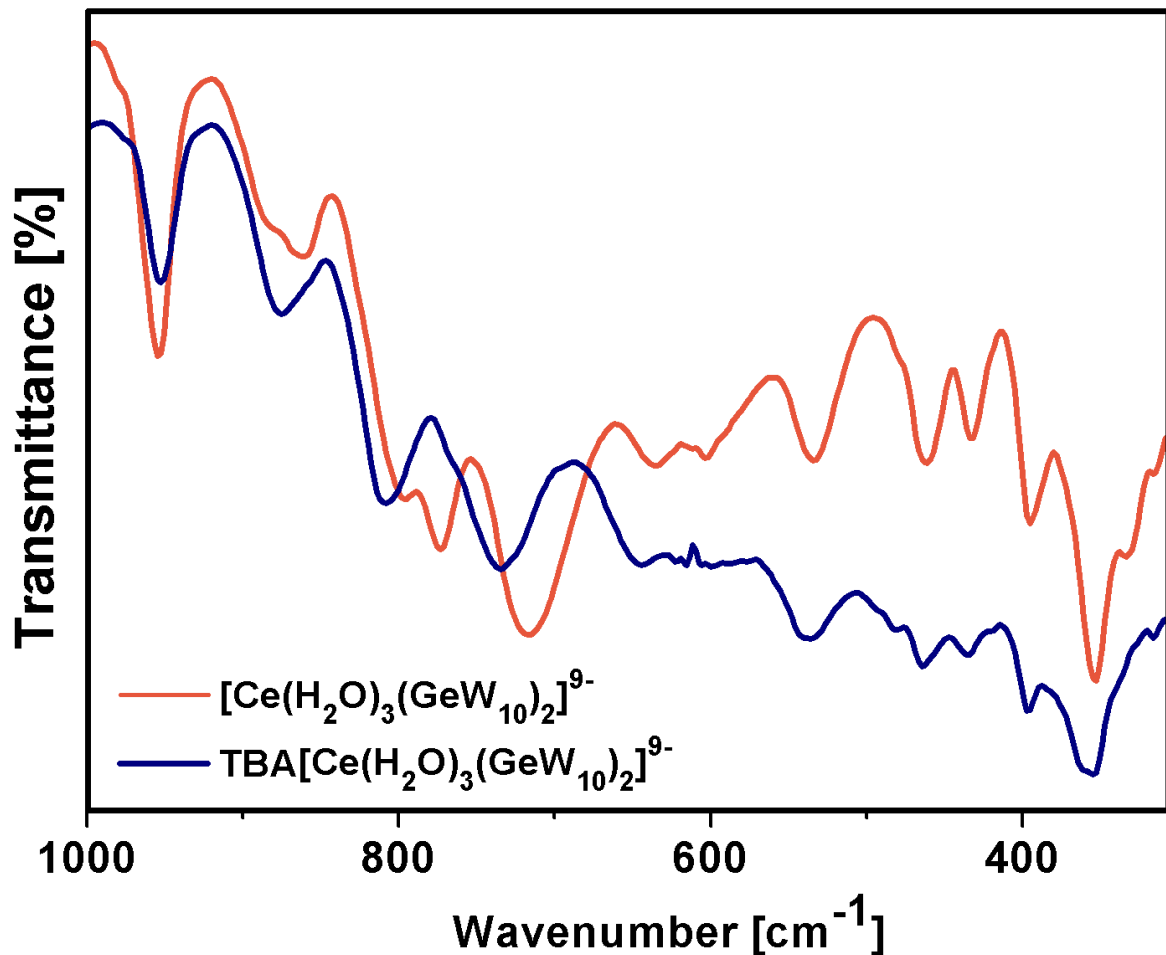


Figure S2. IR-spectra showing the tungsten fingerprint area from 300 - 1000 cm⁻¹ of $[\text{Ce}^{\text{III}}(\text{H}_2\text{O})_3(\text{GeW}_{10})_2]^{9-}$, (orange) and the precipitated polyanion catalyst by addition of tetrabutylammonium bromide after reaction with NPP (NPP = 4-nitrophenylphosphate) or 70 h at 60°C, pD = 7.0 $\text{TBA}[\text{Ce}^{\text{III}}(\text{H}_2\text{O})_3(\text{GeW}_{10})_2]^{9-}$ (royal).

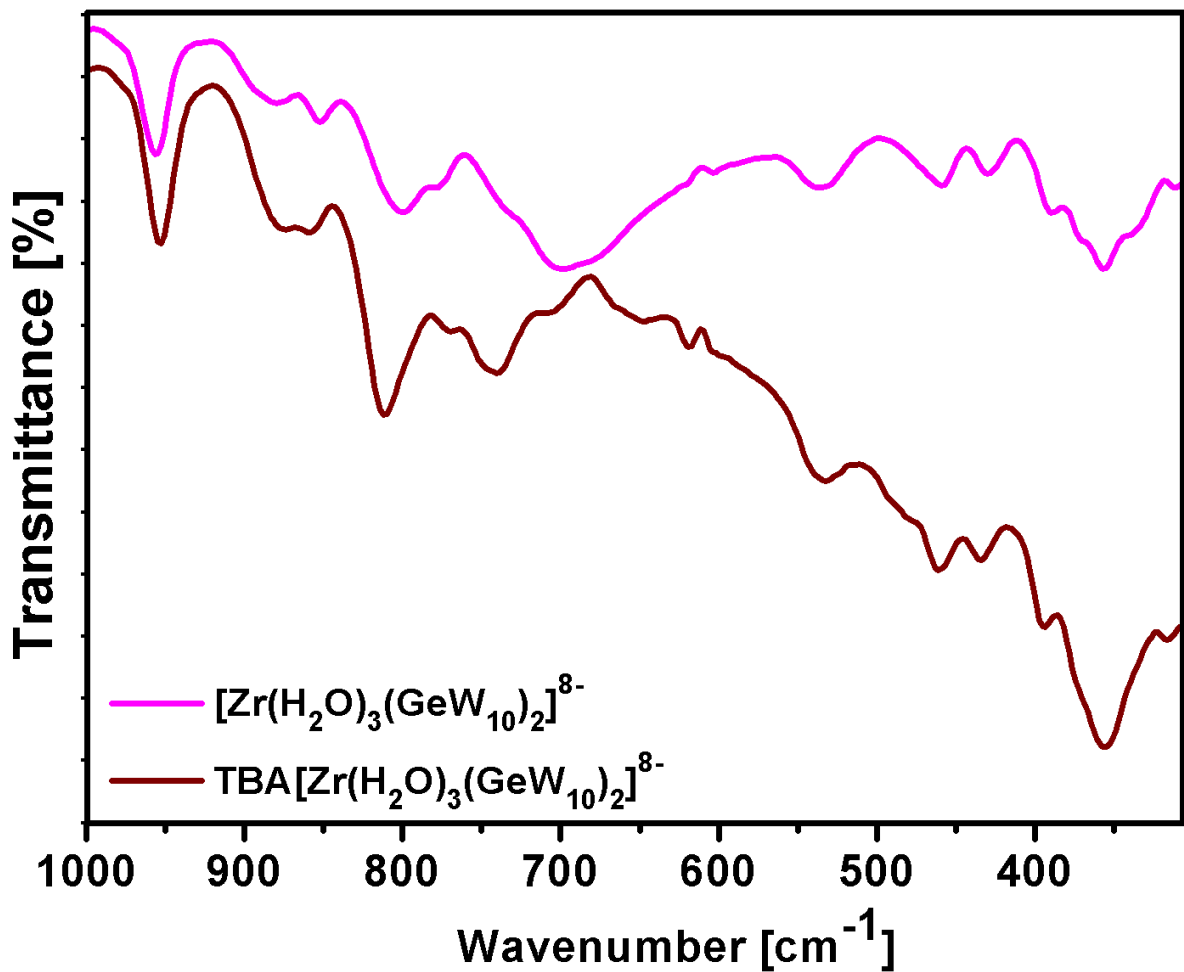


Figure S3. IR-spectra showing the tungsten fingerprint area from 300 - 1000 cm⁻¹ of $[\text{Zr}^{\text{IV}}(\text{H}_2\text{O})_3(\text{GeW}_{10})_2]^{8-}$, (pink) and the precipitated polyanion catalyst by addition of tetrabutylammonium bromide after reaction with NPP (NPP = 4-nitrophenylphosphate) for 70 h at 60°C, pD = 7.0 $\text{TBA}[\text{Zr}^{\text{IV}}(\text{H}_2\text{O})_3(\text{GeW}_{10})_2]^{8-}$ (wine red).

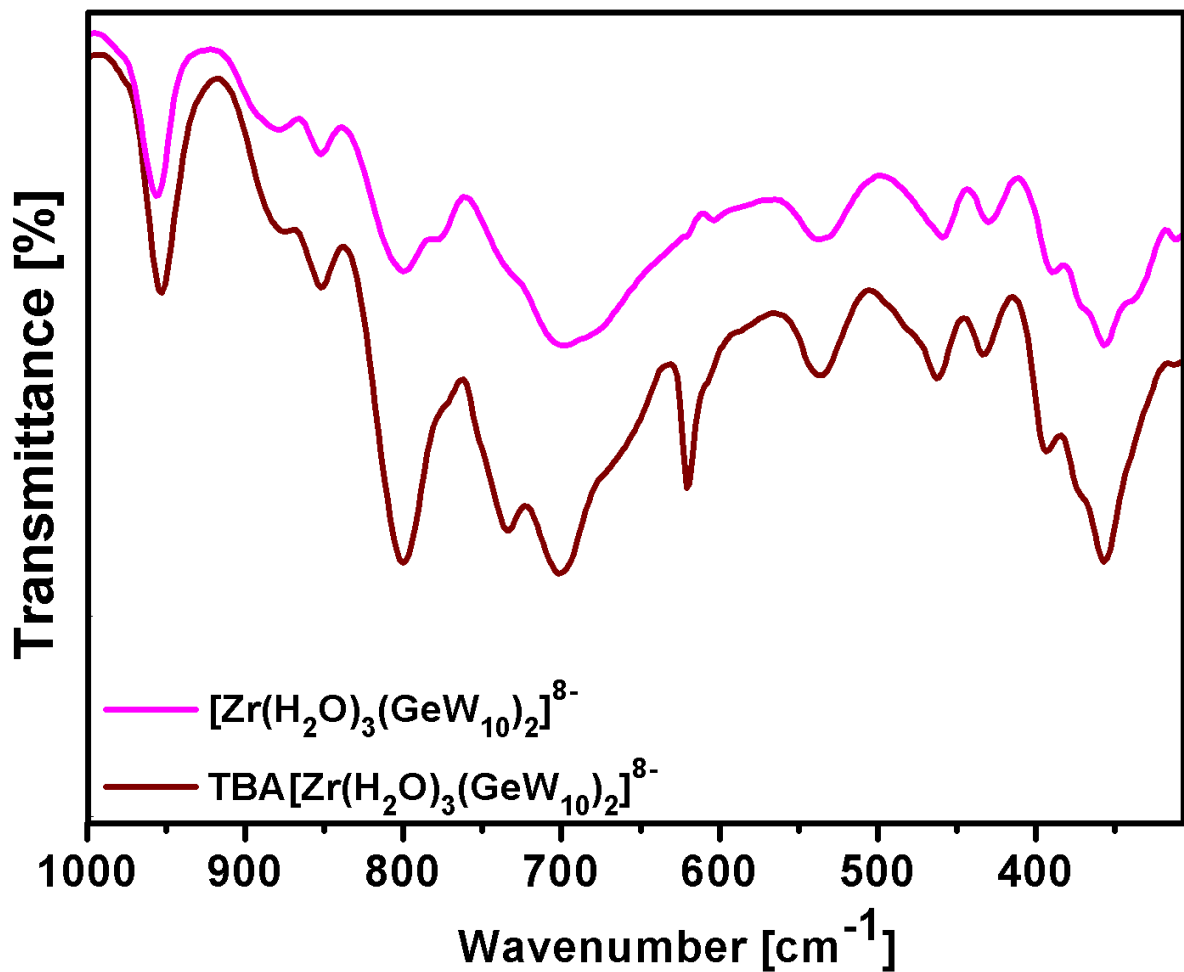


Figure S4. IR-spectra showing the tungsten fingerprint area from 300 - 1000 cm⁻¹ of $[\text{Zr}^{\text{IV}}(\text{H}_2\text{O})_3(\text{GeW}_{10})_2]^{8-}$, (pink) and the precipitated polyanion catalyst by addition of tetrabutylammonium bromide after reaction with DMNP (DMNP = O,O-dimethyl O-(4-nitrophenyl) phosphate) for 100 h at room temperature (25°C), pD = 7.0 $\text{TBA}[\text{Zr}^{\text{IV}}(\text{H}_2\text{O})_3(\text{GeW}_{10})_2]^{8-}$ (wine red).

4. Thermogravimetric Analysis

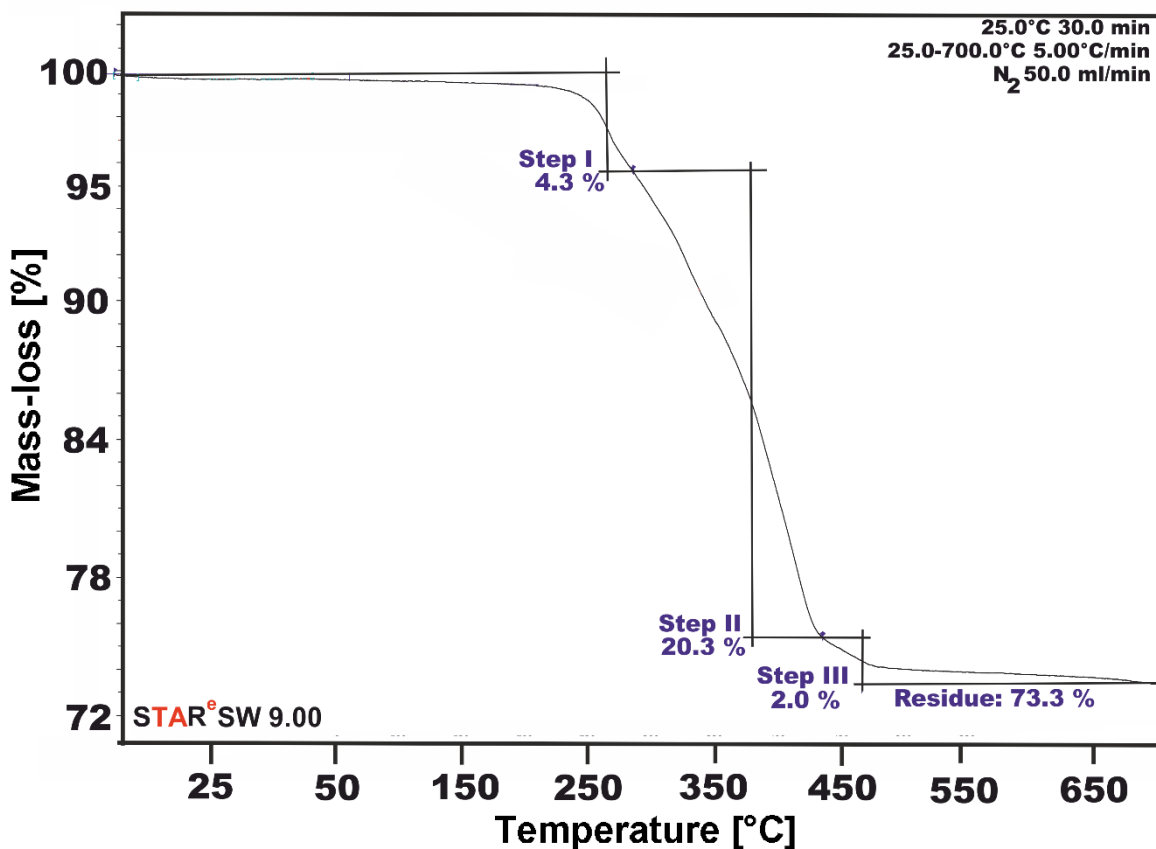


Figure S5. Thermogravimetric curve of $(C_{16}H_{36}N)_7H_2[Ce(H_2O)_3(GeW_{10}O_{35})_2] \cdot 3 (CH_3)_2CO$.

Table S3. TGA results for compound $(C_{16}H_{36}N)_7H_2[Ce(H_2O)_3(GeW_{10}O_{35})_2] \cdot 3 (CH_3)_2CO$. TBA = tetra butyl ammonium $[(n-C_4H_9)_4N]^+$; acetone = $(CH_3)_2CO$.

Step	T, °C	mass-loss, %	number of molecules corresponding to mass-loss
I	20-290	4.3	$3 H_2O + 3$ acetone
II	290-440	20.3	$5 TBA^+$
III	440-700	2.0	$0.5 TBA^+$

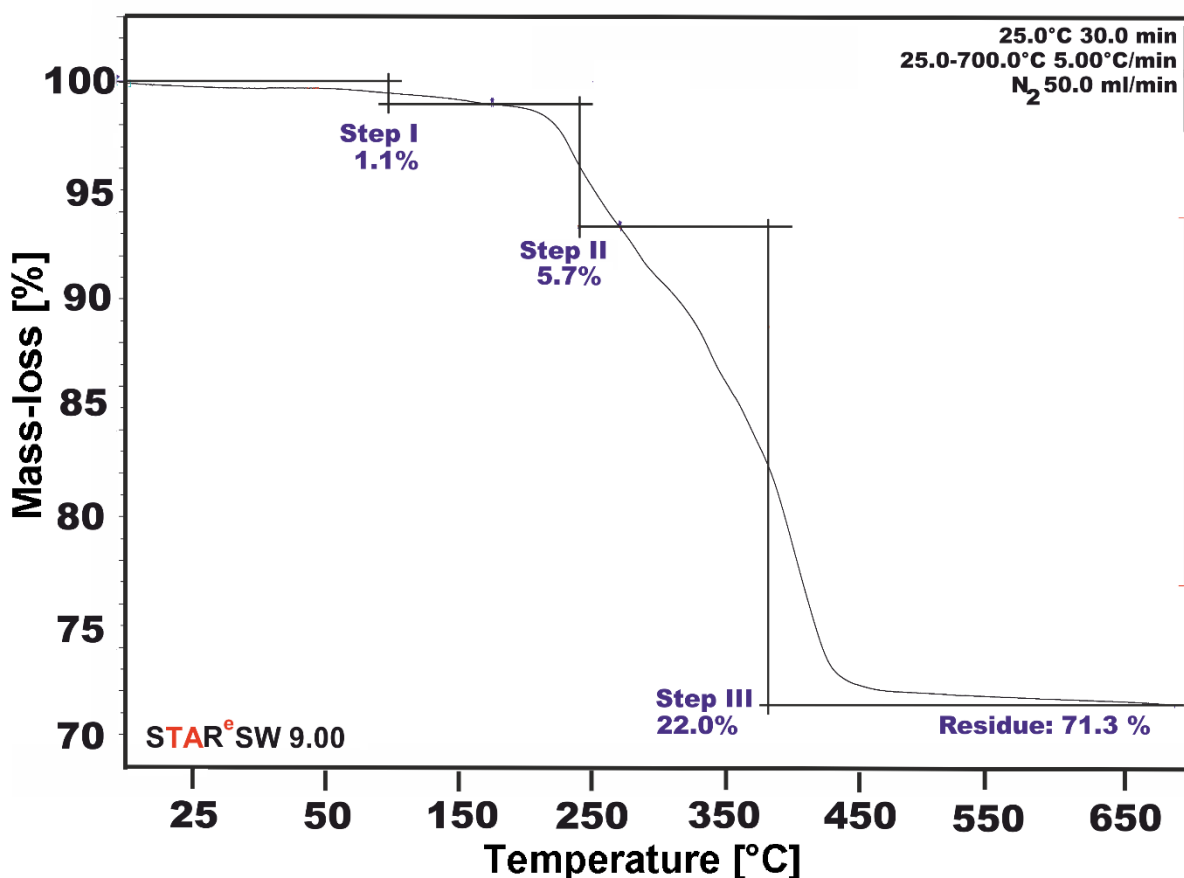


Figure S6. Thermogravimetric curve of $(\text{C}_{16}\text{H}_{36}\text{N})_7\text{H}_2[\text{Nd}(\text{H}_2\text{O})_3(\text{GeW}_{10}\text{O}_{35})_2] \cdot 3 (\text{CH}_3)_2\text{CO}$.

Table S4. TGA results for compound $(\text{C}_{16}\text{H}_{36}\text{N})_7\text{H}_2[\text{Nd}(\text{H}_2\text{O})_3(\text{GeW}_{10}\text{O}_{35})_2] \cdot 3 (\text{CH}_3)_2\text{CO}$. TBA = tetra butyl ammonium $[(n\text{-C}_4\text{H}_9)_4\text{N}]^+$; acetone = $(\text{CH}_3)_2\text{CO}$.

Step	T, °C	mass-loss, %	number of molecules corresponding to mass-loss
I	20-150	1.1	1 acetone
II	150-260	5.7	$\text{TBA}^+ + 2 \text{ acetone} + 3 \text{ H}_2\text{O}$
III	260-700	22.0	6 TBA^+

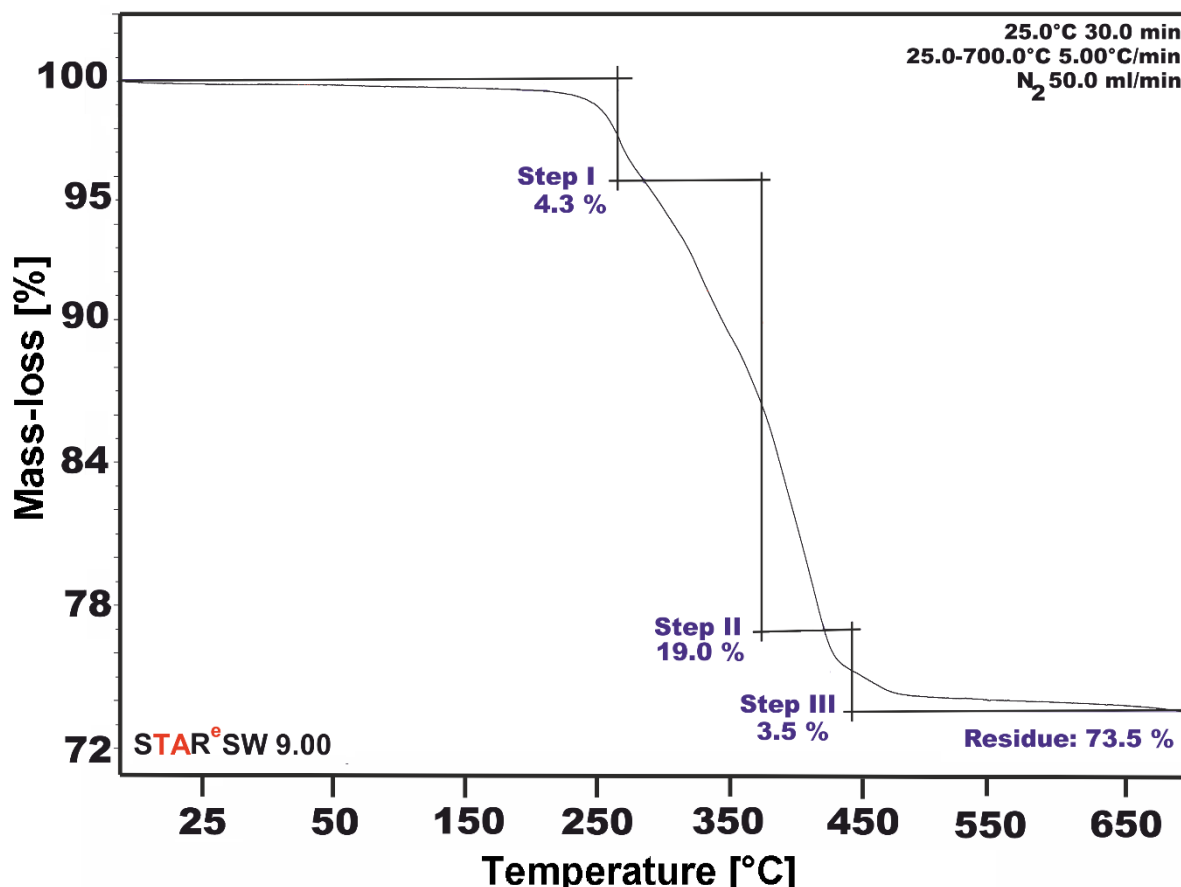


Figure S7. Thermogravimetric curve of $(C_{16}H_{36}N)_7H_2[Er(H_2O)_3(GeW_{10}O_{35})_2] \cdot 3 (CH_3)_2CO$.

Table S5. TGA results for compound $(C_{16}H_{36}N)_7H_2[Er(H_2O)_3(GeW_{10}O_{35})_2] \cdot 3 (CH_3)_2CO$. TBA = tetra butyl ammonium $[(n-C_4H_9)_4N]^+$; acetone = $(CH_3)_2CO$.

Step	T, °C	mass-loss, %	number of molecules corresponding to mass-loss
I	20-280	4.3	3 H ₂ O + 3 acetone
II	280-420	19.0	5 TBA ⁺
III	420-700	3.5	TBA ⁺

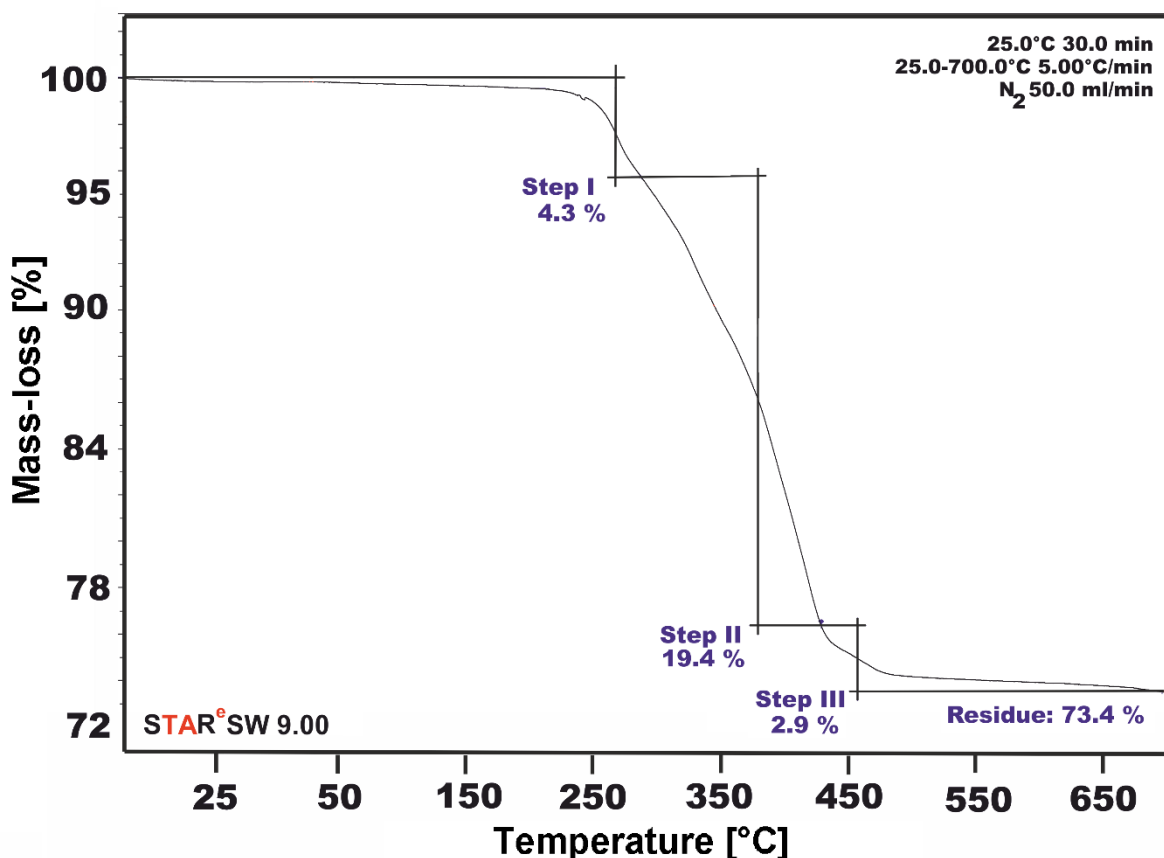


Figure S8. Thermogravimetric curve of $(\text{C}_{16}\text{H}_{36}\text{N})_6\text{H}_2[\text{Zr}(\text{H}_2\text{O})_3(\text{GeW}_{10}\text{O}_{35})_2] \cdot 3 (\text{CH}_3)_2\text{CO}$.

Table S6. TGA results for compound $(\text{C}_{16}\text{H}_{36}\text{N})_6\text{H}_2[\text{Zr}(\text{H}_2\text{O})_3(\text{GeW}_{10}\text{O}_{35})_2] \cdot 3 (\text{CH}_3)_2\text{CO}$. TBA = tetra butyl ammonium $[(n\text{-C}_4\text{H}_9)_4\text{N}]^+$; acetone = $(\text{CH}_3)_2\text{CO}$.

Step	T, °C	mass-loss, %	number of molecules corresponding to mass-loss
I	20-280	4.3	$3 \text{ H}_2\text{O} + 3 \text{ acetone}$
II	280-430	19.4	5 TBA^+
III	430-700	2.9	TBA^+

5. Single-Crystal X-ray Diffraction

Table S7. Experimental parameter and CCDC-Code.

Sample	Machine	Source	Temp.	Detector Distance	Time/Frame	#Frames	Frame width	CCDC
			[K]	[mm]	[s]		[°]	
$[\text{Ce}(\text{H}_2\text{O})_3(\text{GeW}_{10})_2]^{9-}$	Bruker D8	Mo	100	40	40	1856	0.5	1915355
$[\text{Nd}(\text{H}_2\text{O})_3(\text{GeW}_{10})_2]^{9-}$	Bruker D8	Mo	100	40	10	2186	0.5	1915316
$[\text{Er}(\text{H}_2\text{O})_3(\text{GeW}_{10})_2]^{9-}$	Bruker D8	Mo	100	45	28	2541	0.5	1915318
$[\text{Eu}(\text{H}_2\text{O})_3(\text{GeW}_{10})_2]^{9-}$	Bruker D8	Mo	100	52	35	2278	0.5	1915317
$[\text{Zr}(\text{H}_2\text{O})_3(\text{GeW}_{10})_2]^{8-}$	Bruker D8	Mo	100	47	5	2064	0.5	2010882

Table S8. Sample and crystal data of $[\text{Ce}(\text{H}_2\text{O})_3(\text{GeW}_{10})_2]^{9-}$.

Chemical formula	$\text{C}_{121}\text{H}_{278}\text{N}_7\text{O}_{74}\text{CeGe}_2\text{W}_{20}$	Crystal system	monoclinic	
Formula weight [g/mol]	6977.69	Space group	$C_{2/m}$	
Temperature [K]	99.99	Z	8	
Measurement method	\f and \w scans	Volume [\AA³]	40734(6)	
Radiation (Wavelength [\AA])	MoK α ($\lambda = 0.71073$)	Unit cell dimensions [\AA] and [°]	42.057(4)	90.0
Crystal size / [mm³]	0.51 × 0.55 × 0.41		52.117(5)	95.452(3)
Crystal habit	clear orange block		18.6686(17)	90.0
Density (calculated) / [g/cm³]	1.870	Absorption coefficient / [mm⁻¹]	11.800	
Abs. correction Tmin	0.0163	Abs. correction Tmax	0.0439	
Abs. correction type	multi-scan	F(000) [e⁻]	19896.0	

Table S9. Data collection and structure refinement of $[\text{Ce}(\text{H}_2\text{O})_3(\text{GeW}_{10})_2]^{9-}$.

Index ranges	$-50 \leq h \leq 50, -62 \leq k \leq 62, -22 \leq l \leq 22$	Theta range for data collection [°]	4.378 to 50.92	
Reflections number	365094	Data / restraints / parameters	38087/465/1041	
Refinement method	Least squares	Final R indices	all data	$R_1 = 0.1255, wR_2 = 0.2172$
Function minimized	$\Sigma w(F_o^2 - F_c^2)^2$		$I > 2\sigma(I)$	$R_1 = 0.0935, wR_2 = 0.2172$
Goodness-of-fit on F^2	1.010	Weighting scheme	$w=1/[\sigma^2(F_o^2)+(0.0751P)^2+4381.4287P]$	

Largest diff. peak and hole [e Å ⁻³]	3.20/-2.02	where P=(F _o ² +2F _c ²)/3
---	------------	--

Table S10. Sample and crystal data of $[\text{Nd}(\text{H}_2\text{O})_3(\text{GeW}_{10})_2]^{9-}$.

Chemical formula	C ₁₂₁ H ₂₇₈ N ₇ O ₇₄ NdGe ₂ W ₂₀	Crystal system	monoclinic	
Formula weight [g/mol]	6981.81	Space group	C _{2/m}	
Temperature [K]	100.15	Z	8	
Measurement method	\f and \w scans	Volume [Å³]	40946(2)	
Radiation (Wavelength [Å])	MoKα ($\lambda = 0.71073$)	Unit cell dimensions [Å] and [°]	42.1516(13)	90
Crystal size / [mm³]	0.5 × 0.49 × 0.4		52.1970(15)	95.4810(10)
Crystal habit	clear bluish block		18.6956(6)	90
Density (calculated) / [g/cm³]	1.923	Absorption coefficient / [mm⁻¹]	11.774	
Abs. correction Tmin	0.024	Abs. correction Tmax	0.0927	
Abs. correction type	multi-scan	F(000) [e⁻]	20672.0	

Table S11. Data collection and structure refinement of $[\text{Nd}(\text{H}_2\text{O})_3(\text{GeW}_{10})_2]^{9-}$.

Index ranges	-50 ≤ h ≤ 50, -62 ≤ k ≤ 62, -22 ≤ l ≤ 22	Theta range for data collection [°]	4.182 to 50.7	
Reflections number	576991	Data / restraints / parameters	37974/12/1142	
Refinement method	Least squares	Final R indices	all data	R ₁ = 0.1082, wR ₂ = 0.1940
Function minimized	$\Sigma w(F_o^2 - F_c^2)^2$		I>2σ(I)	R ₁ = 0.0706, wR ₂ = 0.1709
Goodness-of-fit on F²	0.975	Weighting scheme	w=1/[σ ² (F _o ²)+(0.0804P) ² +1324.0372P]	
Largest diff. peak and hole [e Å⁻³]	3.31/-3.11		where P=(F _o ² +2F _c ²)/3	

Table S12. Sample and crystal data of $[\text{Er}(\text{H}_2\text{O})_3(\text{GeW}_{10})_2]^{9-}$.

Chemical formula	$\text{C}_{121}\text{H}_{278}\text{N}_7\text{O}_{74}\text{ErGe}_2\text{W}_{20}$	Crystal system	monoclinic	
Formula weight [g/mol]	7004.83	Space group	$P_{21/c}$	
Temperature [K]	100.01	Z	8	
Measurement method	\f and \w scans	Volume [Å³]	38620(3)	
Radiation (Wavelength [Å])	MoKα ($\lambda = 0.71073$)	Unit cell dimension s [Å] and [°]	19.0780(8)	90
Crystal size / [mm³]	$0.51 \times 0.49 \times 0.4$		50.483(2)	97.9686(19)
Crystal habit	clear pink block		40.4902(17)	90
Density (calculated) / [g/cm³]	2.030	Absorption coefficient / [mm⁻¹]	12.648	
Abs. correction Tmin	0.0034	Abs. correction Tmax	0.0192	
Abs. correction type	multi-scan	F(000) [e⁻]	20548.0	

Table S13. Data collection and structure refinement of $[\text{Er}(\text{H}_2\text{O})_3(\text{GeW}_{10})_2]^{9-}$.

Index ranges	-22 ≤ h ≤ 23, -62 ≤ k ≤ 60, -50 ≤ l ≤ 50	Theta range for data collection [°]	4.24 to 52.24	
Reflections number	599247	Data / restraints / parameters	76514/31/2196	
Refinement method	Least squares	Final R indices	all data	$R_1 = 0.1036, wR_2 = 0.2115$
Function minimized			$I > 2\sigma(I)$	$R_1 = 0.0774, wR_2 = 0.1921$
Goodness-of-fit on F^2	1.010	Weighting scheme	$w=1/[\sigma^2(F_o^2)+(0.0912P)^2+1071.9873P]$	
Largest diff. peak and hole [e Å⁻³]	5.75/-5.18		where P=(F _o ² +2F _c ²)/3	

Table S14. Sample and crystal data of $[\text{Eu}(\text{H}_2\text{O})_3(\text{GeW}_{10})_2]^{9-}$.

Chemical formula	$\text{C}_{16}\text{EuGe}_{2.5}\text{NO}_{92}\text{W}_{26}$	Crystal system	monoclinic	
Formula weight [g/mol]	6791.71	Space group	$C_{2/c}$	
Temperature [K]	100.01	Z	8	
Measurement method	\f and \w scans	Volume [Å³]	44825(5)	
Radiation (Wavelength [Å])	MoKα ($\lambda = 0.71073$)	Unit cell dimensions	72.506(5)	90

		[Å] and [°]		
Crystal size / [mm³]	0.52 × 0.5 × 0.46		18.3403(13)	113.711(2)
Crystal habit	clear colorless block		36.816(2)	90
Density (calculated) / [g/cm³]	2.013	Absorption coefficient / [mm⁻¹]	13.932	
Abs. correction Tmin	0.0028	Abs. correction Tmax	0.0192	
Abs. correction type	multi-scan	F(000) [e⁻]	23248.0	

Table S15. Data collection and structure refinement of $[\text{Eu}(\text{H}_2\text{O})_3(\text{GeW}_{10})_2]^{9-}$.

Index ranges	-88 ≤ h ≤ 89, -22 ≤ k ≤ 22, -44 ≤ l ≤ 45	Theta range for data collection [°]	4.334 to 52.262	
Reflections number	524661	Data / restraints / parameters	44559/106/1225	
Refinement method	Least squares	Final R indices	all data	$R_1 = 0.1109, wR_2 = 0.2084$
Function minimized	$\Sigma w(F_o^2 - F_c^2)^2$		$I > 2\sigma(I)$	$R_1 = 0.0707, wR_2 = 0.1783$
Goodness-of-fit on F^2	1.030	Weighting scheme	$w=1/[\sigma^2(F_o^2)+(0.0838P)^2+1437.5043P]$	
Largest diff. peak and hole [e Å⁻³]	3.09/-2.40		where $P=(F_o^2+2F_c^2)/3$	

Table S16. Data collection and structure refinement of $[\text{Zr}(\text{H}_2\text{O})_3(\text{GeW}_{10})_2]^{8-}$.

Chemical formula	C ₁₀₅ H ₂₃₆ N ₆ O ₇₃ ZrGe ₂ W ₂₀	Crystal system	monoclinic	
Formula weight [g/mol]	6664.29	Space group	C _{2/m}	
Temperature [K]	100.0	Z	8	
Measurement method	\f and \w scans	Volume [Å³]	39849(4)	
Radiation (Wavelength [Å])	MoKα ($\lambda = 0.71073$)		42.729(3)	90
Crystal size / [mm³]	0.5 × 0.5 × 0.48		50.160(3)	95.306(3)
Crystal habit	clear colorless block		18.6723(11)	90
Density (calculated) / [g/cm³]	1.944	Absorption coefficient / [mm⁻¹]	11.891	
Abs. correction Tmin	0.0123	Abs. correction Tmax	0.0503	
Abs. correction type	multi-scan	F(000) [e⁻]	20344.0	

Table S17. Data collection and structure refinement of $[\text{Zr}(\text{H}_2\text{O})_3(\text{GeW}_{10})_2]^{8-}$.

Index ranges	-51 ≤ h ≤ 51, -60 ≤ k ≤ 60, -22 ≤ l ≤ 22	Theta range for data collection [°]	4.172 to 50.7	
Reflections number	393904	Data / restraints / parameters	36930/434/1211	
Refinement method	Least squares	Final R indices	all data	$R_1 = 0.1008, wR_2 = 0.2427$
Function minimized	$\Sigma w(F_o^2 - F_c^2)^2$		$I > 2\sigma(I)$	$R_1 = 0.0804, wR_2 = 0.2233$
Goodness-of-fit on F^2	1.029	Weighting scheme	$w=1/[\sigma^2(F_o^2)+(0.1300P)^2+2182.9524P]$	
Largest diff. peak and hole [e Å⁻³]	2.76/-2.46		where $P=(F_o^2+2F_c^2)/3$	

6. Powder X-ray Diffraction (PXRD)

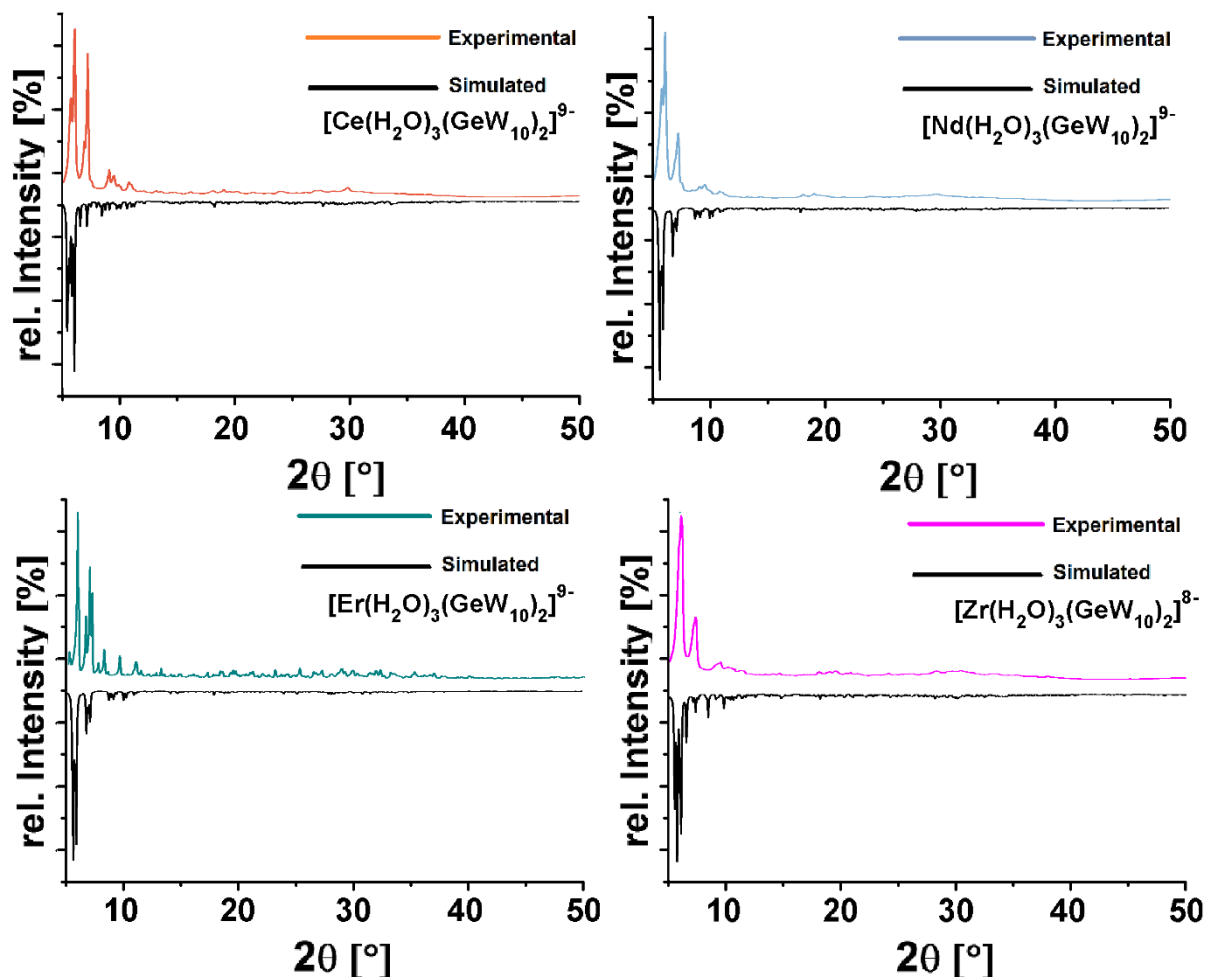


Figure S9. Comparison of the experimental and simulated PXRD patterns of $[\text{M}(\text{H}_2\text{O})_3(\text{GeW}_{10})_2]^n^-$ ($n = 9$ for $\text{M} = \text{Ce}^{\text{III}}$, Nd^{III} , Er^{III} ; $n = 8$ for $\text{M} = \text{Zr}^{\text{IV}}$). Note that differences between the simulated and the experimental PXRD patterns may be due to factors such as scanning speed, preferred orientation, and efflorescence of the crystals, which lose solvent molecules further leading to the collapse of the lattice.

7. UV-Vis Spectroscopy

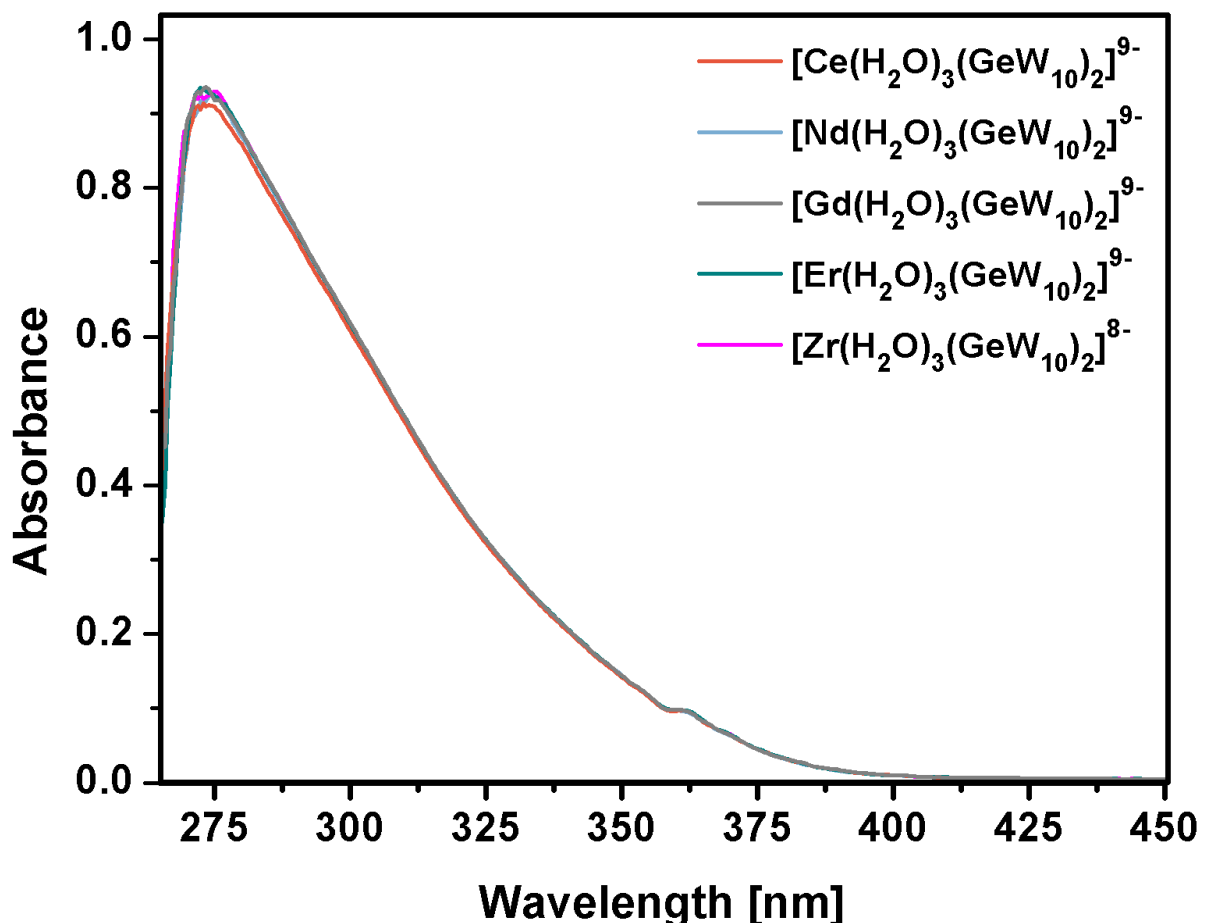


Figure S10. UV/Vis-spectrum of $\text{M}(\text{H}_2\text{O})_3(\text{GeW}_{10})_2$ ($\text{M} = \text{Ce}^{\text{III}}, \text{Nd}^{\text{III}}, \text{Gd}^{\text{III}}, \text{Er}^{\text{III}}, \text{Zr}^{\text{IV}}$) in acetonitrile showing typical O→W ligand-to-metal charge-transfer (275 nm).

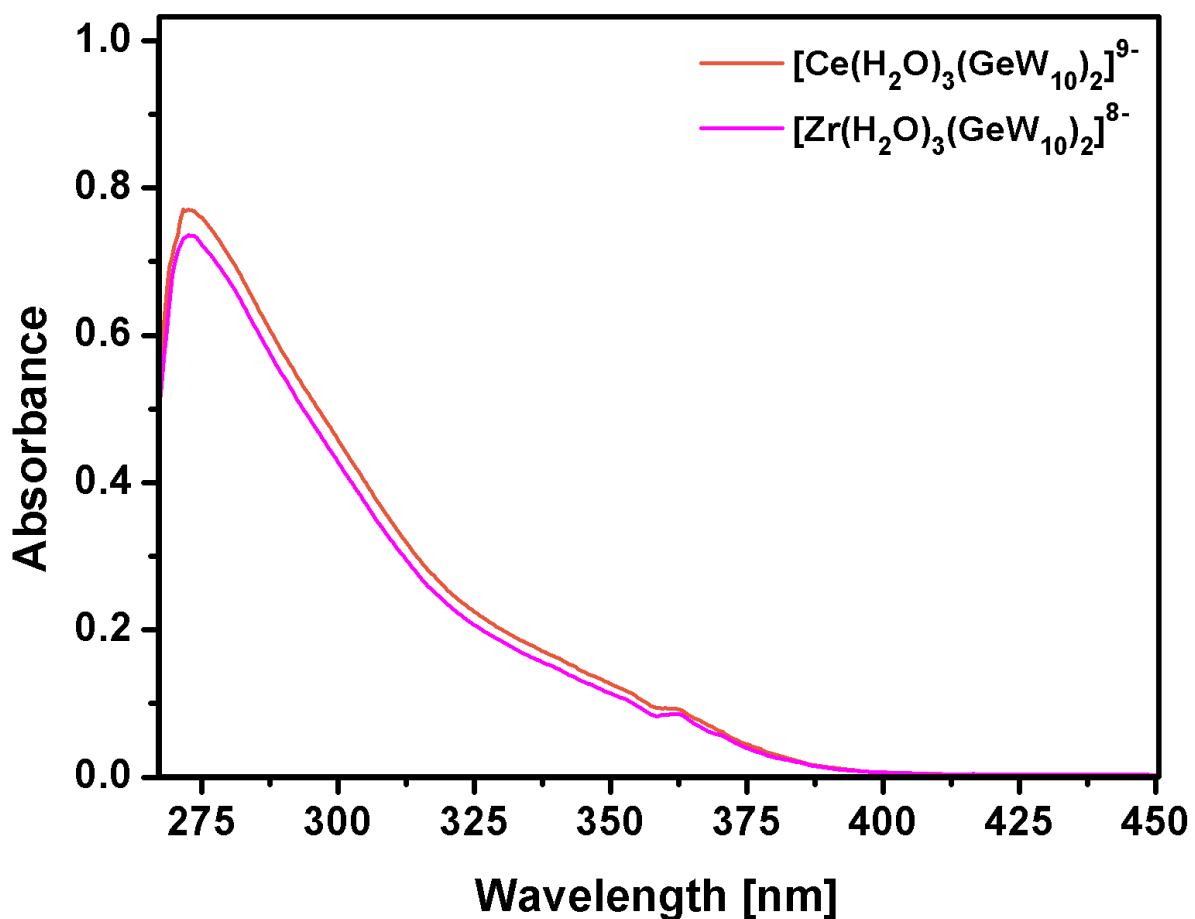


Figure S11. UV/Vis-spectrum of $\text{Na}(\text{Ce}(\text{H}_2\text{O})_3(\text{GeW}_{10})_2)^{9-}$ and $\text{Na}(\text{Zr}(\text{H}_2\text{O})_3(\text{GeW}_{10})_2)^{8-}$ in 125 mM Tris-HCl, pH 7.0 showing typical O \rightarrow W ligand-to-metal charge-transfer (275 nm).

8. Hydrolysis Studies

8.1. Hydrolysis experiments on 4-nitrophenylphosphate (NPP):

Stock solutions of the corresponding POM compound [1 mM] $[\text{Ce}(\text{H}_2\text{O})_3(\text{GeW}_{10}\text{O}_{35})_2]^{9-}$ or $[\text{Zr}(\text{H}_2\text{O})_3(\text{GeW}_{10}\text{O}_{35})_2]^{8-}$ and NPP (2 mM) were prepared in D₂O. After mixing 2.5 mL of each solution in a scintillation vial, the pD value of the solutions was adjusted by the addition of DCI or NaOD. The pD value was calculated using the formula pD = pH + 0.41. The reaction mixtures were heated in a heating block and the reactions followed by means of ¹H NMR spectroscopy after different time intervals. The integration of the peaks corresponding to start, and end products was used to calculate the progress and kinetics of the reaction.

8.2. Hydrolysis experiments on O,O-dimethyl O-(4-nitrophenyl) phosphate (DMNP):

Stock solutions of $[\text{Zr}(\text{H}_2\text{O})_3(\text{GeW}_{10}\text{O}_{35})_2]^{8-}$ [5 mM] and DMNP (8.6 mM) were prepared in Tris-HCl [125 mM]/D₂O (50%) pD 7.0. The pD value was calculated using the formula pD = pH + 0.41. After mixing 2.5 mL of each solution in a vial, the reaction mixture was stirred with 1100 rpm at a constant temperature of 25°C. The progress of the reaction was followed by means of ³¹P NMR spectroscopy after different time intervals. The integration of the peaks corresponding to start, and end products was used to calculate the progress and kinetics of the reaction.

8.3. Recyclability experiment on $[\text{Zr}(\text{H}_2\text{O})_3(\text{GeW}_{10}\text{O}_{35})_2]^{8-}$:

After the end of the first reaction cycle was confirmed by ³¹P-NMR measurements (97% DMNP conversion, Fig. S19), a 100 µL stock solution of DMNP [21.5 mM] was added to the 500 µL NMR-sample containing 2.5 mM of $[\text{Zr}(\text{H}_2\text{O})_3(\text{GeW}_{10}\text{O}_{35})_2]^{8-}$ to obtain a 600 µL sample with the initial ratio $[\text{Zr}(\text{H}_2\text{O})_3(\text{GeW}_{10}\text{O}_{35})_2]^{8-}:\text{DMNP} = 1:1.72$. The reaction mixture was mixed thoroughly by flipping the NMR tube various times and monitored by ³¹P-NMR spectroscopy. Based on the ³¹P-NMR integration values obtained the substrate conversion was calculated.

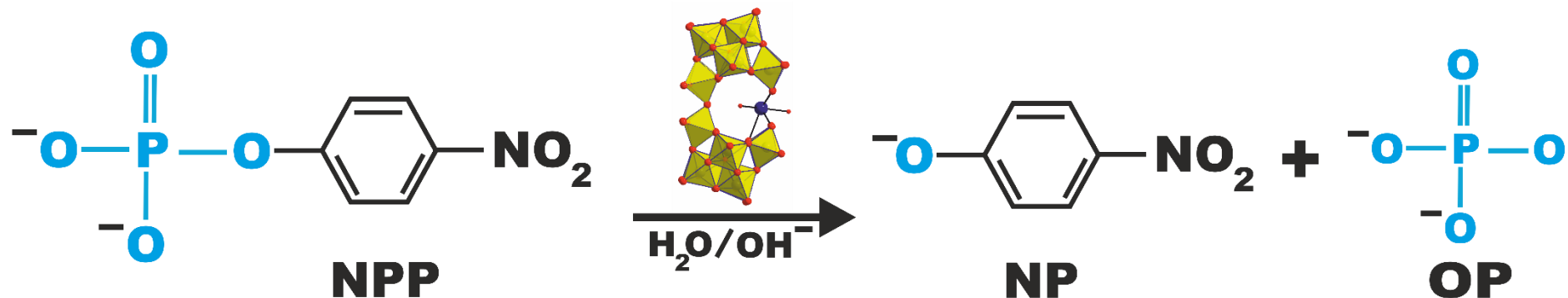
Table S18. Comparison of turnover frequency (TOF) values of $[\text{Zr}(\text{H}_2\text{O})_3(\text{GeW}_{10}\text{O}_{35})_2]^{8-}$ for the first and the second cycle of reaction.

	DMNP conversion (%)	TON	Time [h]	TOF [h ⁻¹]
1 st cycle	57.6	0.99	49.0	0.02
2 nd cycle	53.8	0.93	47.4	0.02

Table S19. General information on the solubility of polyanions $[\text{Ce}(\text{H}_2\text{O})_3(\text{GeW}_{10})_2]^{9-}$ and $[\text{Zr}(\text{H}_2\text{O})_3(\text{GeW}_{10})_2]^{8-}$ in different solvents.

	$[\text{Ce}(\text{H}_2\text{O})_3(\text{GeW}_{10}\text{O}_{35})_2]^{9-}$	$[\text{Zr}(\text{H}_2\text{O})_3(\text{GeW}_{10}\text{O}_{35})_2]^{8-}$
<i>Molecular weight [g/mol]</i>	5343.11	5294.21
<i>Solubility in water [mM]</i>	5.3	5.1
<i>Solubility in DMSO [mM]</i>	15.2	15.5

Scheme S1. Hydrolysis of 4-nitrophenylphosphate (NPP) [1 mM] to p – nitrophenolate (NP) and *ortho* – phosphate (OP) catalyzed by $[\text{M}(\text{H}_2\text{O})_3(\text{GeW}_{10}\text{O}_{35})_2]^{n-}$ ($n = 9$ for $\text{M} = \text{Ce}^{\text{III}}$; $n = 8$ for $\text{M} = \text{Zr}^{\text{IV}}$) [0.5 mM] in D_2O at $\text{pD} 7.0$ and 60° . Blue and red spheres represent the M - and oxygen ions, respectively. Orange for Ge^{IV} and yellow polyhedra for $\{\text{WO}_6\}$.



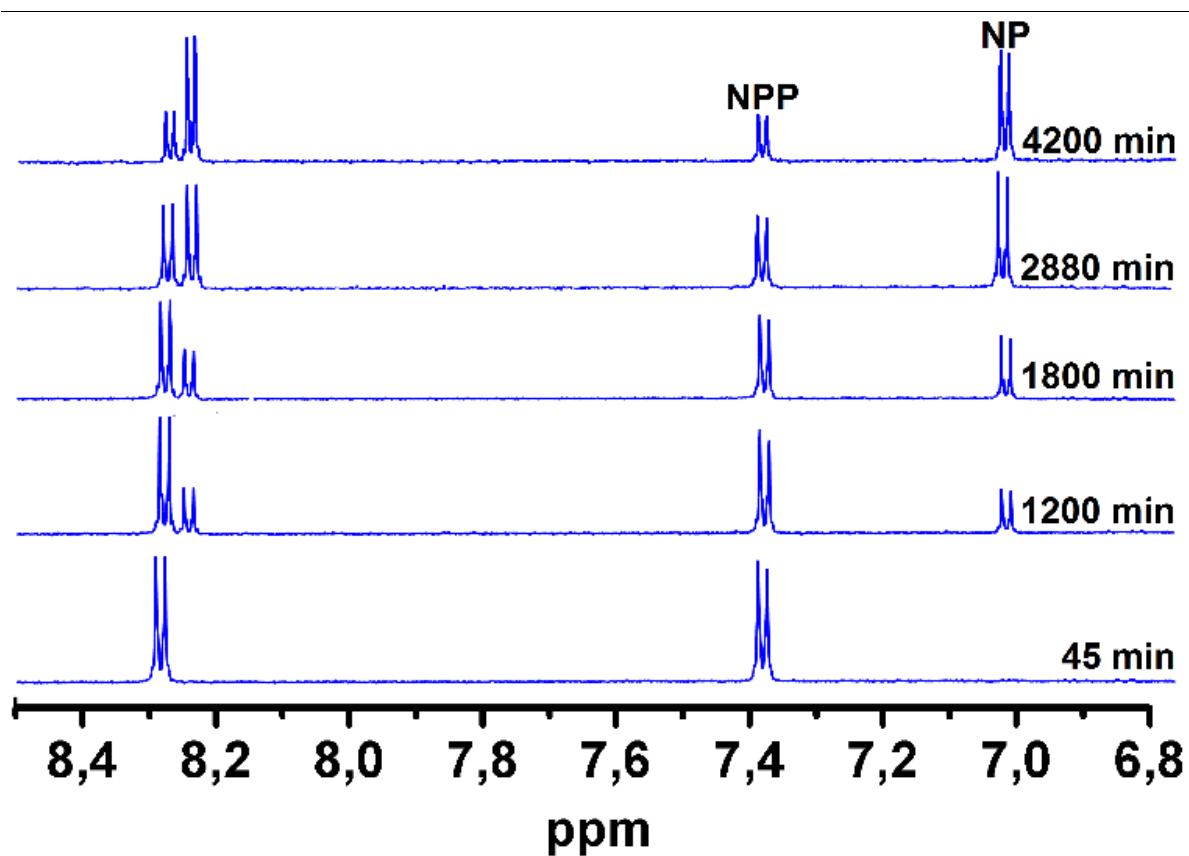


Figure S12. ¹H NMR spectra of the hydrolysis of [1 mM] NPP (NPP = 4-nitrophenylphosphate) to nitrophenol (NP) with $[\text{Ce}(\text{H}_2\text{O})_3(\text{GeW}_{10}\text{O}_{35})_2]^{9-}$ [0.5 mM] in D₂O at pD 7.0 and 60°.

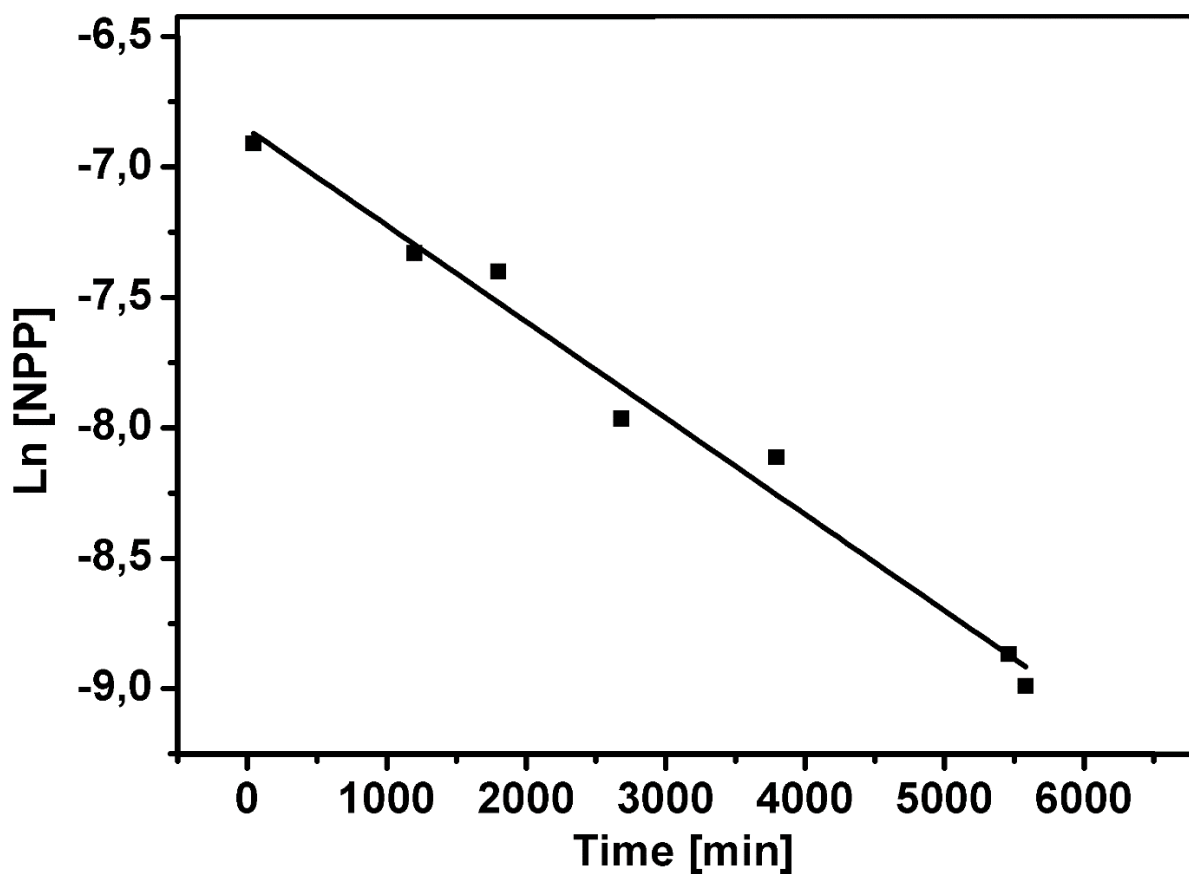


Figure S13. Decrease of 4-nitrophenylphosphate (NPP) concentration as a function of time using the logarithmic 4-nitrophenylphosphate (NPP) concentration values obtained from the NMR integration values after reaction with $[\text{Ce}(\text{H}_2\text{O})_3(\text{GeW}_{10}\text{O}_{35})_2]^{9-}$ at pD 7.0, 60°C for 45, 1200, 1800, 2680, 3790, 5460 and 5580 min. The function is described by the linear fit ($R^2 = 0.97$): $\ln ([\text{NPP}]) = -3.70 (\pm 0.20) \times 10^{-4} x - 6.82$ with x being the reaction time in min. The slope of the linear fit gives the rate constant $k = 3.70 (\pm 0.20) \times 10^{-4} \text{ min}^{-1}$.

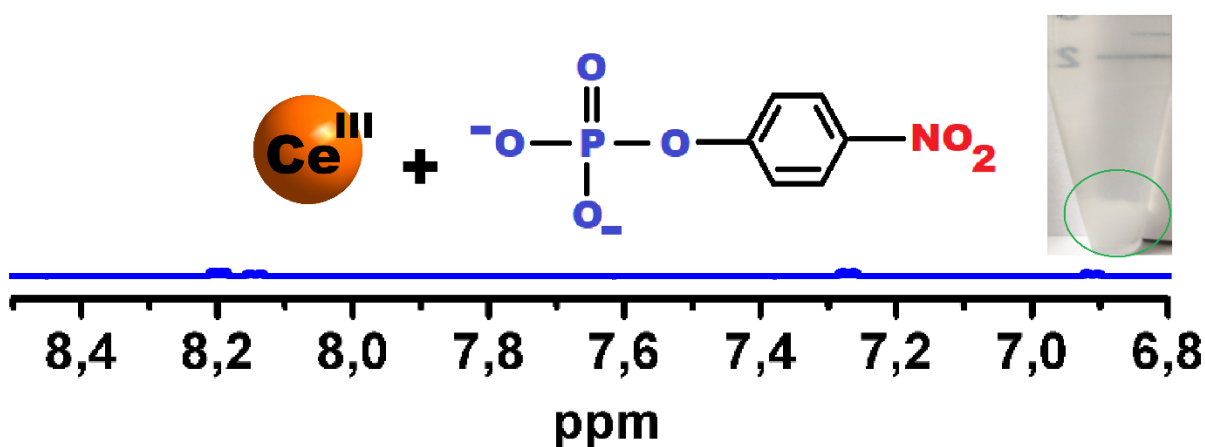


Figure S14. ^1H NMR spectra of 1 mM NPP (NPP = 4-nitrophenylphosphate) in the presence of 0.5 mM $\text{CeCl}_3 \cdot 9 \text{ H}_2\text{O}$ in D_2O (pD = 7.0, 60°C) showing the precipitates formed in the colorless solution.

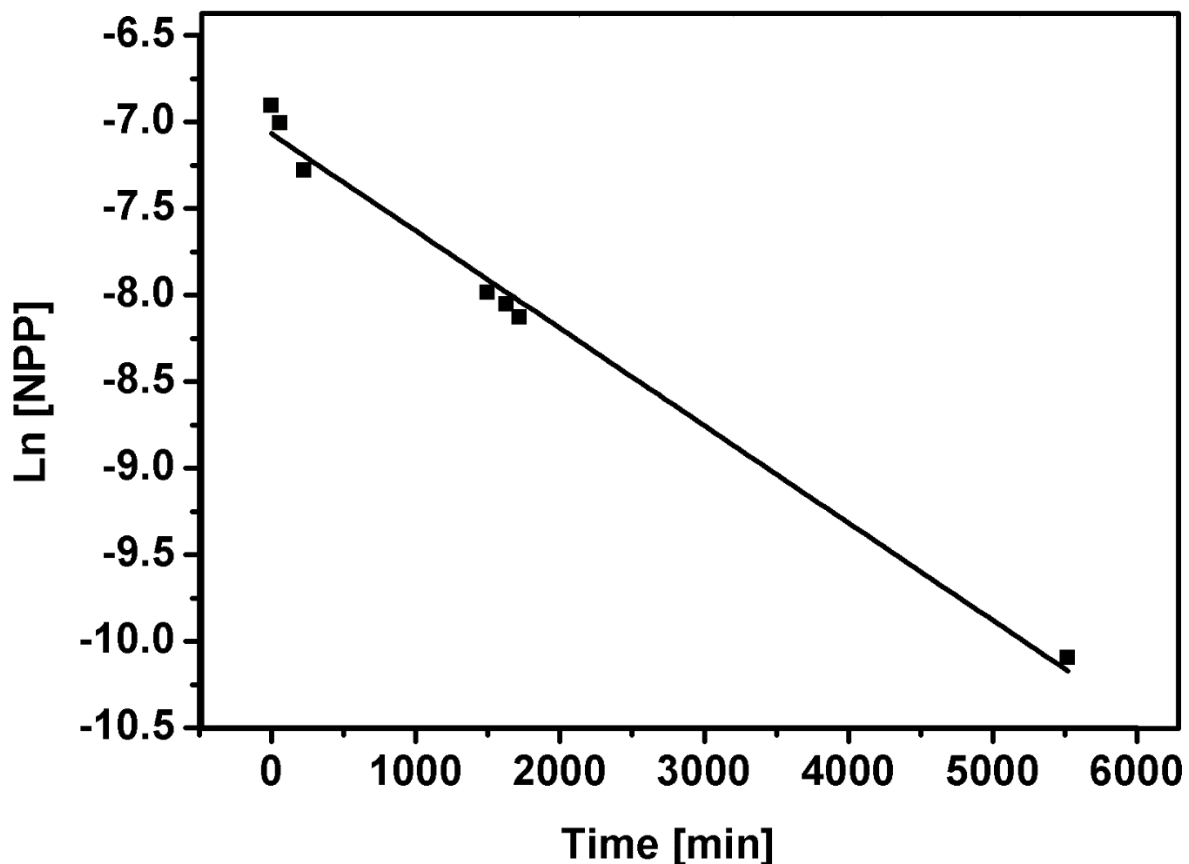


Figure S15. Decrease of 4-nitrophenylphosphate (**NPP**) concentration as a function of time using the logarithmic 4-nitrophenylphosphate (**NPP**) concentration values obtained from the NMR integration values after reaction with $[\text{Zr}(\text{H}_2\text{O})_3(\text{GeW}_{10}\text{O}_{35})_2]^{8-}$ at pD 7.0, 60°C for 60, 225, 1500, 1630, 1720, and 5520 min. The function is described by the linear fit ($R^2 = 0.99$): $\ln ([\text{NPP}]) = -5.62 (\pm 0.10) \times 10^{-4} x - 7.07$ with x being the reaction time in min. The slope of the linear fit gives the rate constant $k = 5.62 (\pm 0.10) \times 10^{-4} \text{ min}^{-1}$.

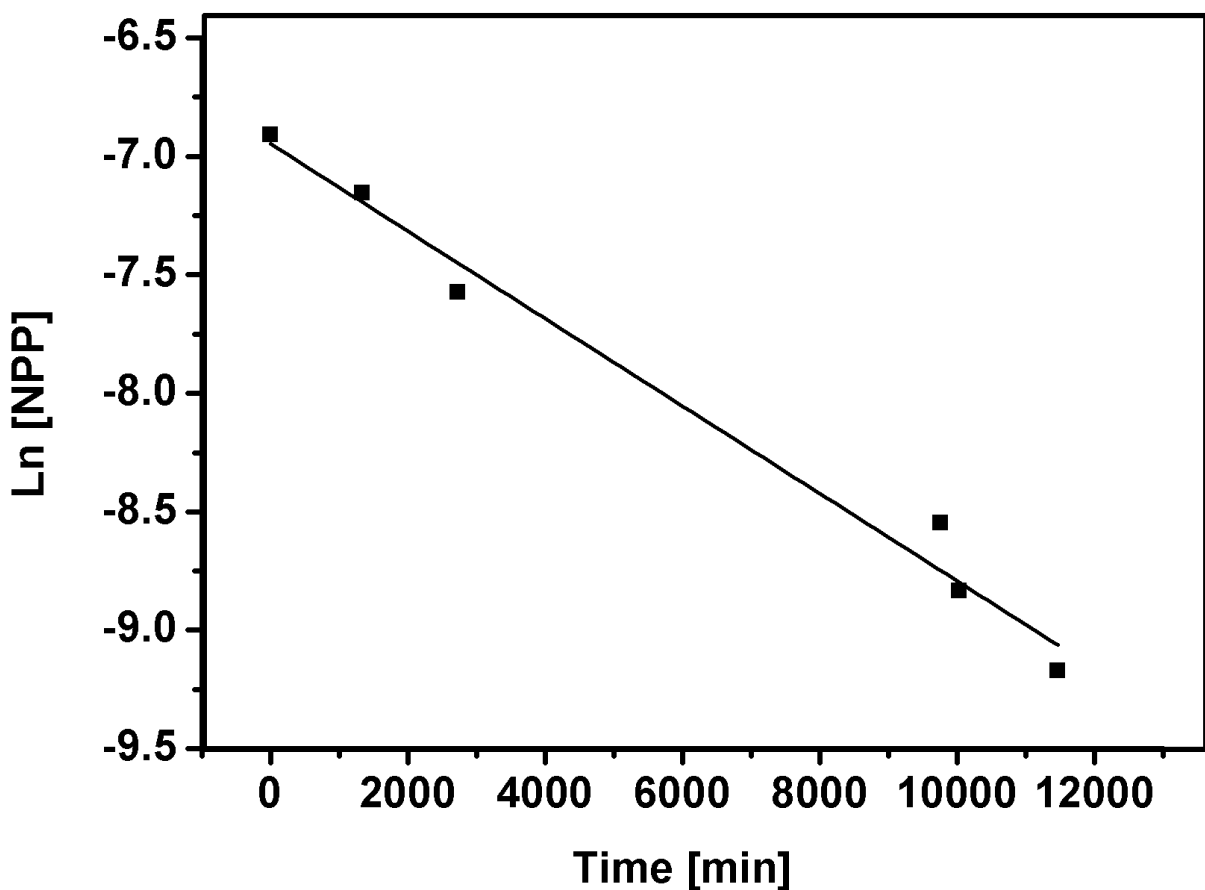
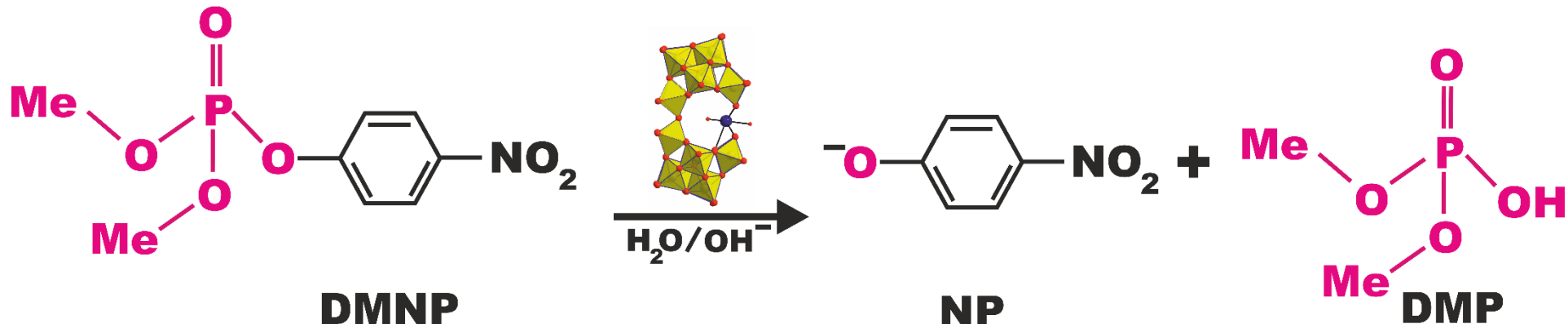
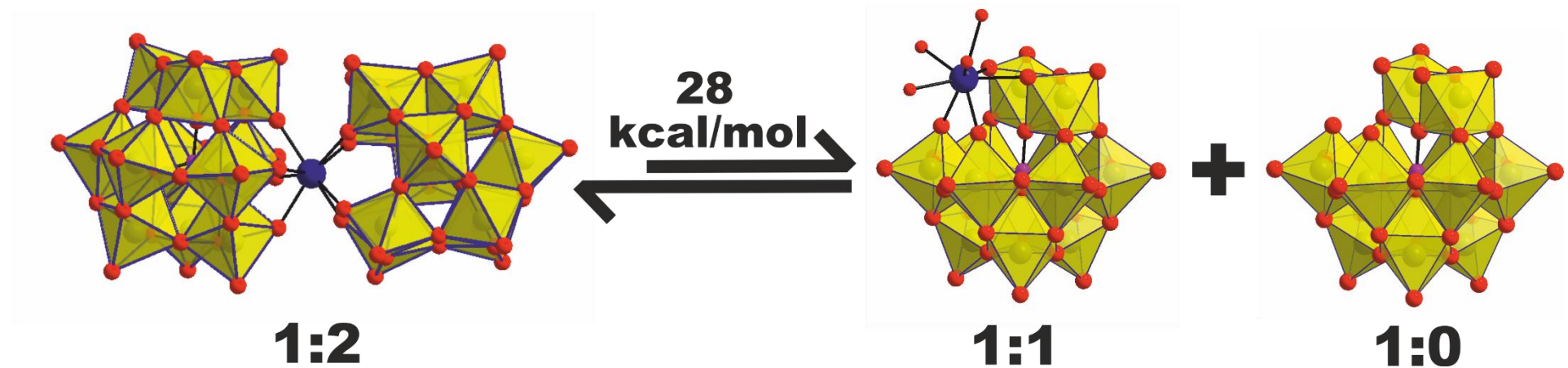


Figure S16. Decrease of 4-nitrophenylphosphate (**NPP**) concentration as a function of time using the logarithmic 4-nitrophenylphosphate (**NPP**) concentration values obtained from the NMR integration values after reaction with $[\text{GeW}_{10}\text{O}_{36}]^{8-}$ at pD 7.0, 60°C for 0, 1335, 2726, 9764, 10028, and 11464 min. The function is described by the linear fit ($R^2 = 0.98$): $\ln ([\text{NPP}]) = -1.85 (\pm 0.12) \times 10^{-4} x - 6.95$ with x being the reaction time in min. The slope of the linear fit gives the rate constant $k = 1.85 (\pm 0.12) \times 10^{-4} \text{ min}^{-1}$.

Scheme S2. Hydrolysis of O,O-dimethyl O-(4-nitrophenyl) phosphate (DMNP) [4.3 mM] to p – nitrophenolate (NP) and dimethyl phosphate (DMP) catalyzed by $[\text{Zr}(\text{H}_2\text{O})_3(\text{GeW}_{10})_2]^{8-}$ [2.5 mM] in Tris-HCl [125 mM] at pD 7.0 and room temperature (25°C). Me = -CH₃. Blue and red spheres represent the Zr^{IV} - and oxygen ions, respectively. Orange for Ge^{IV} and yellow polyhedra for {WO₆}.



Scheme S3. Schematic representation of the thermodynamically unfavored conversion of the dimeric $[\text{Ce}^{\text{III}/\text{IV}}(\text{PW}_{11}\text{O}_{39})_2]^{10/\text{-9-}}$ POM (1:2) to the monomeric $[\text{Ce}^{\text{III}/\text{IV}}\text{PW}_{11}(\text{H}_2\text{O})_2]^{4/\text{-3-}}$ (1:1) species being a crucial step for the POM in order to exhibit hydrolytic activity. Blue and red spheres represent the Ce^{III/IV} - and oxygen ions, respectively. Orange for Ge^{IV} and yellow polyhedra for {WO₆}.



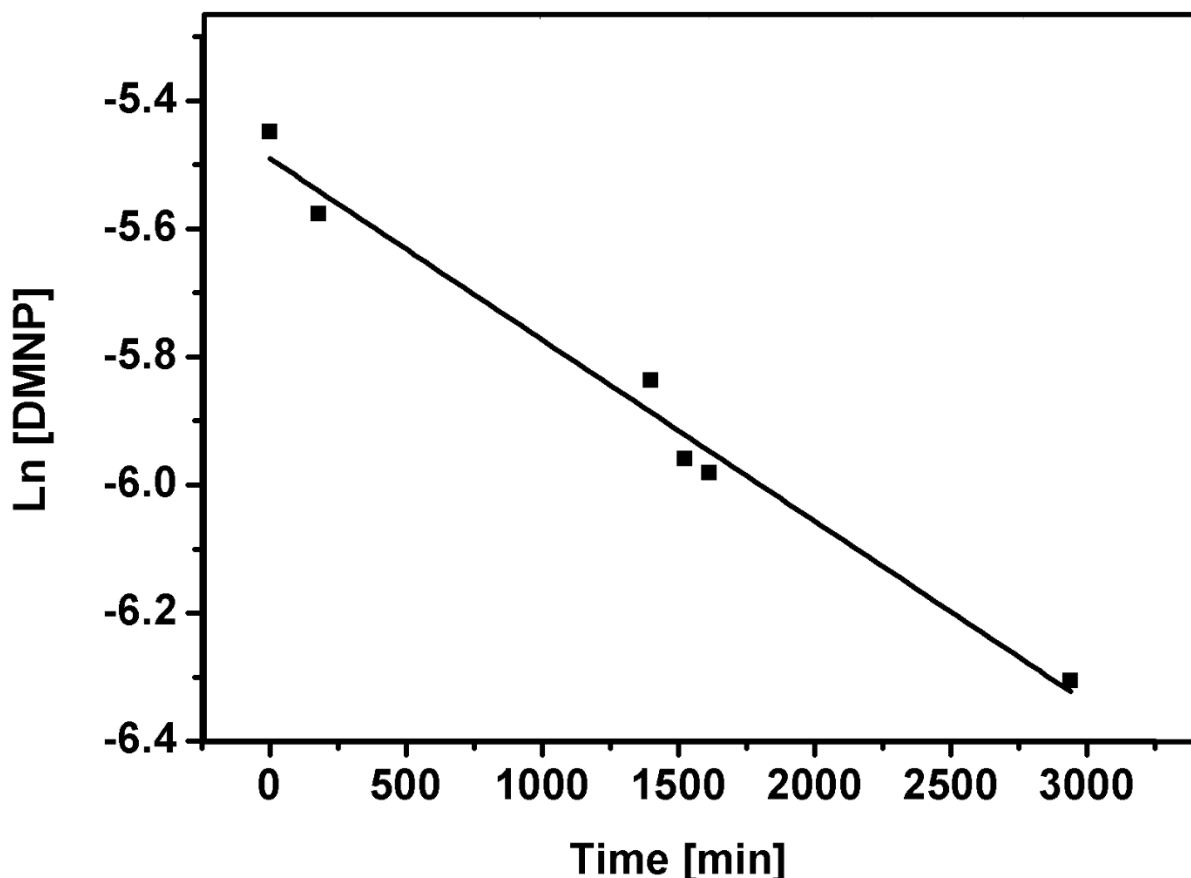


Figure S17. Decrease of O,O-dimethyl O-(4-nitrophenyl) phosphate (**DMNP**) concentration as a function of time using the logarithmic O,O-dimethyl O-(4-nitrophenyl) phosphate (**DMNP**) concentration values obtained from the NMR integration values after reaction with $[\text{Zr}(\text{H}_2\text{O})_3(\text{GeW}_{10}\text{O}_{35})_2]^{8-}$ at pH 7.0, room temperature (25°C) for 180, 1400, 1524, 1614, and 2940 min. The function is described by the linear fit ($R^2 = 0.98$): $\ln ([\text{DMNP}]) = -2.83 (\pm 0.19) \times 10^{-4} x - 5.49$ with x being the reaction time in min. The slope of the linear fit gives the rate constant $k = 2.83 (\pm 0.19) \times 10^{-4} \text{ min}^{-1}$.

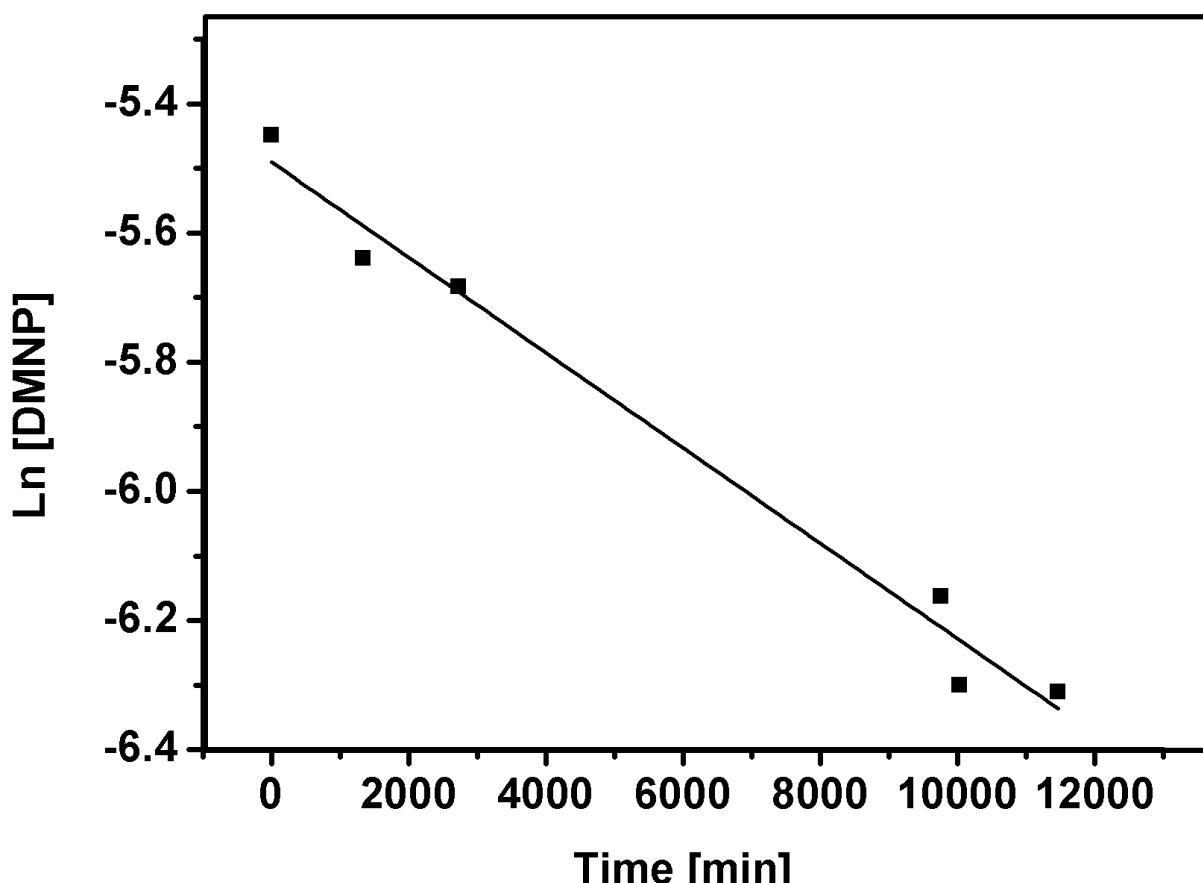


Figure S18. Decrease of O,O-dimethyl O-(4-nitrophenyl) phosphate (DMNP) concentration as a function of time using the logarithmic O,O-dimethyl O-(4-nitrophenyl) phosphate (DMNP) concentration values obtained from the NMR integration values after reaction with $[\text{GeW}_{10}\text{O}_{36}]^{8-}$ at pH 7.0, room temperature (25°C) for 0, 1335, 2726, 9764, 10028, and 11464 min. The function is described by the linear fit ($R^2 = 0.98$): $\ln ([\text{DMNP}]) = -7.38 (\pm 0.48) \times 10^{-5} x - 5.49$ with x being the reaction time in min. The slope of the linear fit gives the rate constant $k = 7.38 (\pm 0.48) \times 10^{-5} \text{ min}^{-1}$.

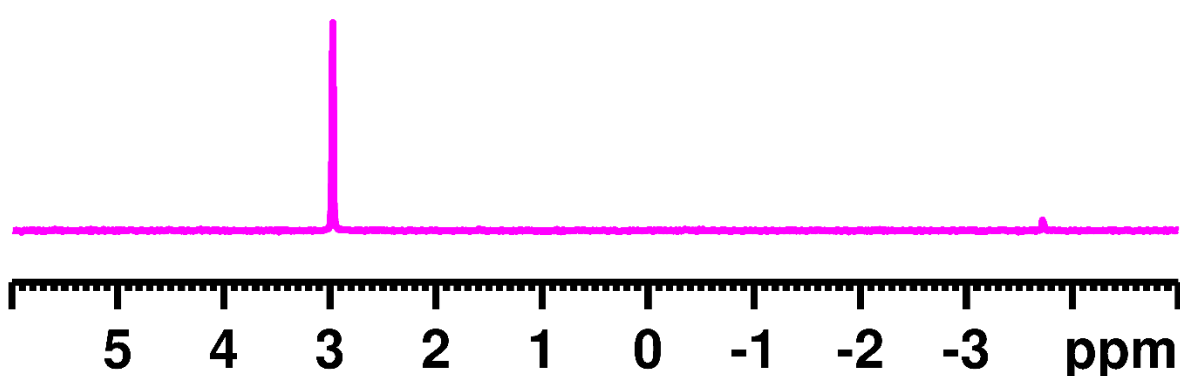


Figure S19. ^{31}P NMR spectrum showing complete hydrolysis of DMNP.

Table S20. Concentration dependent hydrolysis of NPP and DMNP using $[\text{Ce}(\text{H}_2\text{O})_3(\text{GeW}_{10})_2]^{9-}$ and $[\text{Zr}(\text{H}_2\text{O})_3(\text{GeW}_{10})_2]^{8-}$.

POM	Substrate	Concentration [mM]	Time/h	Conversion [%]
$[\text{Ce}(\text{H}_2\text{O})_3(\text{GeW}_{10}\text{O}_{35})_2]^{9-}$	NPP	0.5	45.6	34.78
$[\text{Ce}(\text{H}_2\text{O})_3(\text{GeW}_{10}\text{O}_{35})_2]^{9-}$	NPP	1.0	45.6	49.69
$[\text{Ce}(\text{H}_2\text{O})_3(\text{GeW}_{10}\text{O}_{35})_2]^{9-}$	NPP	1.25	45.6	59.14
$[\text{Ce}(\text{H}_2\text{O})_3(\text{GeW}_{10}\text{O}_{35})_2]^{9-}$	NPP	2.5	45.6	76.23
$[\text{Zr}(\text{H}_2\text{O})_3(\text{GeW}_{10}\text{O}_{35})_2]^{8-}$	DMNP	0.5	49	7.34
$[\text{Zr}(\text{H}_2\text{O})_3(\text{GeW}_{10}\text{O}_{35})_2]^{8-}$	DMNP	1.0	49	28.92
$[\text{Zr}(\text{H}_2\text{O})_3(\text{GeW}_{10}\text{O}_{35})_2]^{8-}$	DMNP	1.25	49	32.46
$[\text{Zr}(\text{H}_2\text{O})_3(\text{GeW}_{10}\text{O}_{35})_2]^{8-}$	DMNP	2.5	49	68.88
$[\text{Zr}(\text{H}_2\text{O})_3(\text{GeW}_{10}\text{O}_{35})_2]^{8-}$	NPP	0.5	25	66.05
$[\text{Zr}(\text{H}_2\text{O})_3(\text{GeW}_{10}\text{O}_{35})_2]^{8-}$	NPP	1.0	25	84.09
$[\text{Zr}(\text{H}_2\text{O})_3(\text{GeW}_{10}\text{O}_{35})_2]^{8-}$	NPP	1.25	25	100

9. Antibacterial Activity

Table S21. Details on the investigated compounds and minimum inhibitory concentration (MIC) of $[\text{Ce}(\text{H}_2\text{O})_3(\text{GeW}_{10})_2]^{9-}$ against *M. catarrhalis* (ATCC 23246)

Compound	MW	c (mM)	m(mg)	mg/ml	V uL/1mL conc. 512 $\mu\text{l}/\text{mL}$	MIC ($\mu\text{g}/\text{ml}$)
$[\text{Ce}(\text{H}_2\text{O})_3(\text{GeW}_{10})_2]^{9-}$	5343.11	1.887	5	10.0	51.20	32
$\text{Ce}(\text{NO}_3)_3$	434.22	23.030	12	10.0	51.20	>256
$[\text{GeW}_{10}\text{O}_{36}]^{8-}$	2907.9	3.439	10	10.0	51.20	64
azithromycin						0.125
ciprofloxacin						<0.06

Table S22. Details on the investigated compounds and minimum inhibitory concentration (MIC) of $[\text{Zr}(\text{H}_2\text{O})_3(\text{GeW}_{10})_2]^{8-}$ against *M. catarrhalis* (ATCC 23246).

Compound	MW	c (mM)	m(mg)	mg/ml	V uL/1ml conc. 512 $\mu\text{l}/\text{mL}$	MIC ($\mu\text{g}/\text{mL}$)
$[\text{Zr}(\text{H}_2\text{O})_3(\text{GeW}_{10})_2]^{8-}$	5294.21	1.897	6.69	10.0	51.20	16
$\text{ZrO}(\text{NO}_3)_2$	434.22	40.161	24.19	10.0	51.20	16
azithromycin						0.06

10. References

- 1 K. Sugahara, T. Kimura, K. Kamata, K. Yamaguchi, N. Mizuno. *Chem. Commun.* **2012**, *48*, 8422-8424.
- 2 Bruker SAINT v7.68A Copyright © 2005-2016 Bruker AXS.
- 3 G. M. Sheldrick SADABS University of Göttingen, Germany (1996).
- 4 G. M. Sheldrick, (1996) SHELXS. University of Göttingen, Germany.
- 5 G. M. Sheldrick, (1996) SHELXL. University of Göttingen, Germany.
- 6 O. V. Dolomanov, L. J. Bourhis, R. J. Gildea, J. A. K. Howard, H. Puschmann. OLEX2. *J. Appl. Cryst.* **2009**, *42*, 339-341.
- 7 C. B. Huebschle, G. M. Sheldrick, B. Dittrich. ShelXle: a Qt graphical user interface for SHELXL. *J. Appl. Cryst.* **2011**, *44*, 1281-1284.
- 8 Clinical Laboratory Standard Institute CLSI. 2009. Methods for dilution antimicrobial susceptibility tests for bacteria that grow aerobically. Approved standard-Eight edition.M07-A8. Clinical Laboratory Standards Institute, Wayne, Pa.
- 9 Y. Kikukawa, K. Yamaguchi, N. Mizuno. Sandwich-Type Zinc-Containing Polyoxometalates with a Hexaprismane Core $[\{Zn_2W(O)O_3\}_2]^{4+}$ Synthesized by Thermally Induced Isomerization of a Metastable Polyoxometalate. *Inorg. Chem.* **2010**, *49*, 8194-8196.
- 10 K. Suzuki, Y. Kikukawa, S. Uchida, H. Tokoro, K. Imoto, S. Ohkoshi, N. Mizuno. Three-Dimensional Ordered Arrays of $58 \times 58 \times 58 \text{ \AA}^3$ Hollow Frameworks in Ionic Crystals of M_2Zn_2 -Substituted Polyoxometalates. *Angew. Chem. Int. Ed.* **2012**, *51*, 1597 –1601.
- 11 K. Suzuki, M. Shinoe, N. Mizuno. Synthesis and Reversible Transformation of Cu_n -Bridged ($n = 1, 2, \text{ or } 4$) Silicodecatungstate Dimers. *Inorg. Chem.* **2012**, *51*, 11574–11581.

-
- 12 K. Suzuki, M. Sugawa, Y. Kikukawa, K. Kamata, K. Yamaguchi, N. Mizuno. Strategic Design and Refinement of Lewis Acid–Base Catalysis by Rare-Earth-Metal-Containing Polyoxometalates. *Inorg. Chem.* **2012**, *51*, 6953–6961.
- 13 T. Hirano, K. Uehara, K. Kamata, N. Mizuno. Palladium(II) Containing γ -Keggin Silicocatungstate That Efficiently Catalyzes Hydration of Nitriles. *J. Am. Chem. Soc.* **2012**, *134*, 6425–6433.
- 14 Y. Kikukawa, Y. Kuroda, K. Yamaguchi, N. Mizuno. Diamond-Shaped $[Ag_4]^{4+}$ Cluster Encapsulated by Silicotungstate Ligands: Synthesis and Catalysis of Hydrolytic Oxidation of Silanes. *Angew. Chem. Int. Ed.* **2012**, *51*, 2434–2437.
- 15 Y. Kikukawa, K. Suzuki, M. Sugawa, T. Hirano, K. Kamata, K. Yamaguchi, N. Mizuno. Cyanosilylation of Carbonyl Compounds with Trimethylsilyl Cyanide Catalyzed by an Yttrium-Pillared Silicotungstate Dimer. *Angew. Chem. Int. Ed.* **2012**, *51*, 3686–3690.
- 16 Y. Kikukawa, K. Suzuki, K. Yamaguchi, N. Mizuno. Synthesis, Structure Characterization, and Reversible Transformation of a Cobalt Salt of a Dilacunary γ -Keggin Silicotungstate and Sandwich-Type Di- and Tetracobalt-Containing Silicotungstate Dimers. *Inorg. Chem.* **2013**, *52*, 8644–8652.
- 17 Y. Kikukawa, Y. Kuroda, K. Suzuki, M. Hibino, K. Yamaguchi, N. Mizuno. A discrete octahedrally shaped $[Ag_6]^{4+}$ cluster encapsulated within silicotungstate ligands. *Chem. Commun.* **2013**, *49*, 376–378.
- 18 Y. Kuriyama, Y. Kikukawa, K. Suzuki, K. Yamaguchi, N. Mizuno. Water- and Temperature-Triggered Reversible Structural Transformation of Tetranuclear Cobalt (II) Cores Sandwiched by Polyoxometalates. *Chem. Eur. J.* **2016**, *22*, 3962–3966.
- 19 K. Suzuki, F. Tang, Y. Kikukawa, K. Yamaguchi, N. Mizuno. Visible-Light-Induced Photoredox Catalysis with a Tetracerium Containing Silicotungstate. *Angew. Chem. Int. Ed.* **2014**, *53*, 5356–5360.
- 20 R. Sato, K. Suzuki, T. Minato, M. Shinoe, K. Yamaguchi, N. Mizuno. Field-induced slow magnetic relaxation of octahedrally coordinated mononuclear Fe(III)-, Co(II)-, and Mn(III)-containing polyoxometalates. *Chem. Commun.* **2015**, *51*, 4081–4084.

-
- 21 K. Suzuki, T. Hanaya, R. Sato, T. Minato, K. Yamaguchi, N. Mizuno. Hexanuclear tin(II) and mixed valence tin(II,IV) oxide clusters within polyoxometalates. *Chem. Commun.* **2016**, *52*, 10688–10691.
- 22 T. Hanaya, K. Suzuki, R. Sato, K. Yamaguchi, N. Mizuno. Creation of bismuth–tungsten oxide nanoclusters using lacunary polyoxometalates. *Dalton Trans.* **2017**, *46*, 7384–7387.
- 23 K. Suzuki, R. Sato, T. Minato, M. Shinoe, K. Yamaguchi, N. Mizuno. A cascade approach to hetero-pentanuclear manganese-oxide clusters in polyoxometalates and their single-molecule magnet properties. *Dalton Trans.* **2015**, *44*, 14220–14226.
- 24 R. Sato, K. Suzuki, T. Minato, K. Yamaguchi, N. Mizuno. Sequential Synthesis of 3d–3d'–4f Heterometallic Heptanuclear Clusters in between Lacunary Polyoxometalates. *Inorg. Chem.* **2016**, *55*, 2023–2029.
- 25 K. Yonesato, H. Ito, H. Itakura, D. Yokogawa, T. Kikuchi, N. Mizuno, K. Yamguchi, K. Suzuki. Controlled Assembly Synthesis of Atomically Precise Ultrastable Silver Nanoclusters with Polyoxometalates. *J. Am. Chem. Soc.* **2019**, *141*, 19550–19554.
- 26 T. Minato, D. Aravena, E. Ruiz, K. Yamaguchi, N. Mizuno. Effect of Heteroatoms on Field-Induced Slow Magnetic Relaxation of Mononuclear Fe^{III} ($S = 5/2$) Ions within Polyoxometalates. *Inorg. Chem.* **2018**, *57*, 6957–6964.
- 27 J. Miao, S. Zhang, S.–J. Li, Y.–H. Gao, X. Zhang, X.–N. Wang, S.–X. Liu. pH-Controlled assembly of two polyoxometalate chains based on $[\alpha\text{-GeW}_{11}\text{O}_{39}]^{8-}$ and Eu³⁺: syntheses, crystal structures, and properties. *J. Coord. Chem.* **2011**, *64*, 4006–4015.
- 28 R. Gupta, F. Hussain, J. N. Behera, A. M. Bossoh, I. M. Mbomekalle, P. de Oliveira. Syntheses, crystal structure, electrochemistry and luminescence properties of lanthan–germanotungstates. *RSC Adv.* **2015**, *5*, 99754–99765.
- 29 F. Hussain, S. Sandriesser, M. Speldrich, G. R. Patzke. A new series of lanthanoid containing Keggin-type germanotungstates with acetate chelators: $\{[\text{Ln}(\text{CH}_3\text{COO})\text{GeW}_{11}\text{O}_{39}(\text{H}_2\text{O})]_2\}^{12-}$ {Ln = Eu^{III}, Gd^{III}, Tb^{III}, Dy^{III}, Ho^{III}, Er^{III}, Tm^{III}, and Yb^{III}}. *J. Solid State Chem.* **2011**, *184*, 214–219.

-
- 30 J. Wang, Q. Yan, X. Du, X. Duan, J. Niu. Synthesis, crystal structures and properties of three rare earth substituted germanotungstates: M/[α -GeW₁₁O₃₉] (M = Nd, Eu, and Tb) *Inorg. Chim. Acta* **2008**, *361*, 2701–2706.
- 31 J. Wang, X. Du, Q. Yan, J. Niu. Synthesis, structure and properties of rare earth substituted germanotungstates: Pr/[α -GeW₁₁O₃₉]. *J. Coord. Chem.* **2008**, *61*, 3467-3475.
- 32 Z. Li, X.-X. Li, S.-T. Zheng. Three-dimensional architectures based on 1:1 type lanthanide-substituted Keggin-type polyoxometalates and lanthanide cations. *Inorg. Chem. Commun.* **2017**, *80*, 27-32.
- 33 J.-P. Wang, X.-Y. Duan, X.-D. Du, J.-Y. Niu. Novel Rare Earth Germanotungstates and Organic Hybrid Derivatives: Synthesis and Structures of M/[α -GeW₁₁O₃₉] (M = Nd, Sm, Y, Yb) and Sm/[α -GeW₁₁O₃₉] (DMSO). *Cryst. Growth Des.* **2006**, *6*, 2266 – 2270.
- 34 Y-G. Li, L. Xu, G. G. Gao, N. Jiang, H. Liu, F. Y. Li, Y. Y. Yang. New fabrication of lanthanide complexes based on the polyoxometalate ligand of the [α (1,4)-GeW₁₀O₃₈]¹²⁻ anion. *Cryst. Eng. Comm.* **2009**, *11*, 1512–1514.
- 35 A. S. Mougharbel, S. Bhattacharya, B. S. Bassil, A. Rubab, J. van Leusen, P. Kögerler, J. Wojciechowski, U. Kortz. Lanthanide-Containing 22-Tungsto-2-germanates [Ln(GeW₁₁O₃₉)₂]¹³⁻: Synthesis, Structure, and Magnetic Properties. *Inorg. Chem.* **2020**, *59*, 4340-4348.
- 36 K.-Y. Wang, B. S. Bassil, Z. Lin, I. Römer, S. Vanhaecht, T. N. Parac-Vogt, C. S. de Pipaon, J. R. Galan-Mascaros, L. Fan, J. Cao, U. Kortz. Ln₁₂-Containing 60-Tungstogermanates: Synthesis, Structure, Luminescence, and Magnetic Studies. *Chem. Eur. J.* **2015**, *21*, 18168–18176.
- 37 B. Artetxe, S. Reinoso, L. S. Felices, L. Lezama, J. M. Gutierrez-Zorrilla, J. A. Garcia, J. R. Galan-Mascaros, A. Haider, U. Kortz, C. Vicent. Cation-Directed Dimeric versus Tetrameric Assemblies of Lanthanide-Stabilized Dilacunary Keggin Tungstogermanates. *Chem. Eur. J.* **2014**, *20*, 12144–12156.

-
- 38 B. Artetxe, S. Reinoso, L. S. Felices, J. R. Gutierrez-Zorrilla, J. A. Garcia, F. Haso, T. Liu, C. Vicent. Crown-Shaped Tungstogermanates as Solvent-Controlled Dual Systems in the Formation of Vesicle-Like Assemblies. *Chem. Eur. J.* **2015**, *21*, 7736–7745.
- 39 S. Reinoso, M. J. Marques, J. R. Galan-Mascaros, P. Victoria, J. R. Gutierrez-Zorrilla. Giant Crown-Shaped Poly tungstate Formed by Self-Assembly of Ce^{III}-Stabilized Dilacunary Keggin Fragments. *Angew. Chem. Int. Ed.* **2010**, *49*, 8384–8388.
- 40 B. S. Bassil, M. H. Dickman, I. Römer, B. von der Kammer, U. Kortz. The Tungstogermanate $[Ce_{20}Ge_{10}W_{100}O_{376}(OH)_4(H_2O)_{30}]^{56-}$: A Polyoxometalate Containing 20 Cerium(III) Atoms. *Angew. Chem. Int. Ed.* **2007**, *46*, 6192–6195.
- 41 R. Khoshnavazi, S. Gholamyan. Sandwich-type polyoxoanions based on A- β -GeW₉. Synthesis and characterization of $[(A-\beta\text{-GeW}_9O_{34})_2(MOH_2)_3CO_3]^{13-}$ (M = Y³⁺, Sm³⁺, and Yb³⁺) polyoxoanions. *J. Coord. Chem.* **2010**, *63*, 3365–3372.
- 42 S. S. Mal, N. H. Nsouli, M. Carraro, A. Sartorel, G. Scorrano, H. Oelrich, L. Walder, M. Bonchio, U. Kortz. Peroxo-Zr/Hf-Containing Undecatungstosilicates and -Germanates. *Inorg. Chem.* **2010**, *49*, 7–9
- 43 L. Chen, L. Li, B. Liu, G. Xue, H. Hu, F. Fu, J. Wang. A zirconium-containing sandwich-type dimer based on trivacant α - and β -[GeW₉O₃₄]¹⁰⁻ units, $[Zr_3O(OH)_2(\alpha\text{-GeW}_9O_{34})(\beta\text{-GeW}_9O_{34})]^{12-}$. *Inorg. Chem. Commun.* **2009**, *12*, 1035–1037
- 44 L. Huang, S.-S. Wang, J.-W. Zhao, L. Cheng, G.-Y. Yang. Synergistic Combination of Multi-Zr^{IV} Cations and Lacunary Keggin Germanotungstates Leading to a Gigantic Zr₂₄-Cluster-Substituted Polyoxometalate. *J. Am. Chem. Soc.* **2014**, *136*, 7637–7642
- 45 Z.-H. Ni, Z. Zhang, G.-Y. Yang. Two New Tetra-Zr(IV)-Substituted Sandwich-Type Polyoxometalates Functionalized by Different Organic Amine Ligands. *J. Clust. Sci.* **2018**, *29*, 1185–1191.
- 46 Z.-H. Ni, H.-L. Li, X.-Y. Li, G. -Y. Yang. Zr₄-Substituted polyoxometalate dimers decorated by d-tartaric acid/glycolic acid: syntheses, structures and optical/electrochemical properties. *Cryst. Eng. Comm.* **2019**, *21*, 876–883.

-
- 47 Z. Zhang, H.-L. Li, Y.-L. Wang, G.-Y. Yang. Syntheses, Structures, and Electrochemical Properties of Three New Acetate-Functionalized Zirconium-Substituted Germanotungstates: From Dimer to Tetramer. *Inorg. Chem.* **2019**, *58*, 2372–2378.
- 48 Z. Zhang, Y.-L. Wang, G.-Y. Yang. Two inorganic-organic hybrid polyoxotungstates constructed from tetra-Zr^{IV}-substituted sandwich-type germanotungstates functionalized by tris ligand. *Inorg. Chem. Commun.* **2017**, *85*, 32-36.